Excotic ground states in the honeycomb J_1-J_2 Heisenberg model

Daniel Guerreiro Holmedal

Excotic ground states in the honeycomb J_1-J_2 Heisenberg model

Daniel Guerreiro Holmedal

Excotic ground states in the honeycomb J_1-J_2 Heisenberg model

Abstract

In this work, new sets of multi-q ground states of the honeycomb J_1-J_2 Heisenberg model in the case of $J_1 = 2J_2$ were found by rewriting the Hamiltonian in a way that allows for a geometric interpretation of the ground states of the J_1-J_2 honeycomb Heisenberg model. It was then investigated whether these new obtained multi-q ground states are competitive with the spin spiral ground states favoured by quantum fluctuations in a low temperature environment. This was achieved by calculating the partition function of the classical perturbations of the multi-q ground states. The numerical evaluation reveals that Coplanar states are more likely of being realized at low temperatures than non-coplanar states, and among the coplanar states, the colinear states have the highest probability of being realized at low temperatures. The most favoured co-linear ground state is also a single-q spin spiral ground state which has previously been found to be the spin spiral ground state favoured by quantum fluctuations.

1

Takk

Jeg vil takke min veileder Olav Syljåsen for alle våre verdifulle diskusjoner, hans tålmodighet og for at han alltid hadde tid til meg. Han har lært meg mye i løpet av denne oppgaven.

Jeg vil også takke de ansatte og mine medstudenter ved teoretisk fysikk for gode samtaler, og et godt og inkluderende studentmiljø.

Contents

1 Introduction

Magnetic materials consists of atoms bonded together by electrons. These electrons each have a spin, which gives rise to a magnetic momentum around the electrons. The pairwise interactions between the spins in the material have an energy cost associated to them, which causes the internal energy of the material to depend on the state of the spins. The magnetic properties of the material is therefore largely governed by the possible states of the spins in the material as well as their corresponding energy cost. At low temperatures, the ground states largely governs the behaviour of the system. In the case of all magnetic materials, the ground state is found by minimizing all pairwise interactions between the spins in the material. In the case of ferromagnetic materials, this is done by aligning the spins in the same direction. Anti-ferromagnetic materials however, minimize the energy by having the spins align in opposite directions. Some anti-ferromagnetic materials are frustrated, meaning that it is impossible to simultaneously minimize all pairwise interactions between the spins, which gives rise to a large amount of degenerate ground states. This frustration is of academic interest as it has been shown to be an important mechanism in high temperature superconductors [11, 1]. Frustrated magnets also give rise to interesting low temperature phase transitions such as spin liquid phases [2].

The Heisenberg model is widely used to study magnetic materials where the electrons are strongly bonded to the atoms, and the atoms are bonded together through covalent bonds. In this case, the total spin of the electrons in the valance bond of the atoms is important for the behaviour of the material. If the sum of the spins is $S = 1/2$, the material behaves as a quantum system. When the total spin of the valence bond electrons increases, the quantum effects diminish, and the system can be approximated as a classical system. An example of a frustrated honeycomb anti-ferromagnet with total spin $(S = 3/2)$ is $Bi_3Mn_4O_12(NO_3)$[10].

Finding the ground states of a frustrated Heisenberg model has been shown to be very difficult to do analytically. One commonly used method is the Luttinger-Tisza method [6, 5], that reduces the number of Lagrange multipliers used when minimizing the energy. The resulting Lagrange multipliers then yields a set of equations which must be satisfied by all ground states, but are not sufficient to guarantee a ground state. A well studied set of solutions to the Luttinger-Tisza method on two dimensional lattices, are the single-q spin spiral states. These states are coplanar states that only have a single contributing Fourier mode. In many cases, these are not the only ground states of the system, as there might exist states with multiple contribut-

ing Fourier modes (multi-q). These multi-q states are however largely unknown, and therefore little is known about their contribution to the behaviour of frustrated magnetic systems. A known example of such multi-q states is the Skyrmion lattice state [8, 9].

At low temperatures, the state which minimizes the free energy of the system will be realized. Consequently, ground states with a high number of surrounding low energy fluctuations will have a higher probability of being realized. Mulder et al. (2010)[7] investigated the single-q spin spiral ground states of the honeycomb J_1-J_2 Heisenberg model, where the spin spiral ground states favoured by quantum fluctuations were mapped out. In the present work, new multi-q ground states of the honeycomb J_1-J_2 Heisenberg model will be investigated. The aim of this investigation is to see whether these new multi-q ground states are competitive with the favoured spin spiral ground states described in Mulder et al. (2010)[7] in a low temperature environment. This will be achieved by utilizing a method developed by Balla. et. al. (2019) [3] to rewrite the Hamiltonian in a way that allows for a geometric interpretation of the ground states of the J_1-J_2 honeycomb Heisenberg model. This way, a parameterized set of new ground states is identified. The entropy of the classical fluctuations around the ground states will then be calculated and compared to the spin spiral ground states in order to identify the ground states with higher probability of being realized at low temperatures.

2 Crystalline structures

A large portion of solid substances are crystalline, which means that the atoms or molecules are structured in a lattice. Since the electromagnetic force depends on the distance between particles, it is natural that the properties of the solid largely depends on the properties of its lattice. The simplest type of lattices are known as Bravais lattices. In a Bravais lattice, all lattice points are equivalent in the sense that their surroundings are equal. In three dimensions, a Bravais lattice is defined through three linearly independent vectors $\mathbf{a}_1$, $\mathbf{a}_2$, and $\mathbf{a}_3$, which are known as the primitive vectors of the lattice. Any lattice point $\mathbf{p}$ can then be associated with three unique integers l, m, and n, such that $\mathbf{p} = l\mathbf{a}_1 + m\mathbf{a}_2 + n\mathbf{a}_3$. An example of a Bravais lattice is the cubic lattice, which has the primitive vectors

$$\mathbf{a}_1 = (1,0,0), \quad \mathbf{a}_2 = (0,1,0), \quad \mathbf{a}_3 = (0,0,1) \tag{1}$$

where the lattice spacing, the distance between lattice points, has been chosen to be unity. In two dimensions only two primitive vectors are needed. An example of a two dimensional Bravais lattice is the triangular lattice, which has primitive vectors

$$\mathbf{a}_1 = (1,0), \quad \mathbf{a}_2 = \frac{1}{2}(1,\sqrt{3}) \tag{2}$$

Many crystalline materials do not have such a simple Bravais lattice structure. An example of this is graphene, where the underlying crystalline structure is the honeycomb lattice. The honeycomb lattice can be constructed by defining the two lattice points $\mathbf{p}_0 = (0,0)$ and $\mathbf{p}_1 = (0, 1/\sqrt{3})$, and then using the primitive vectors in eq. (2) to construct the two triangular Bravais lattices that arise from adding multiples of the primitive vectors to p_0 and p_1. Figure 1 shows the construction of the honeycomb lattice, where $\mathbf{R}$ is the vector translating from $\mathbf{p}_0$ to $\mathbf{p}_1$.

A general crystalline structure is defined through a cluster of points $\{p_i\}$, which is known as the basis of the lattice, and the primitive translation vectors $\mathbf{a}_1$, $\mathbf{a}_2$, and $\mathbf{a}_3$. Any point $\mathbf{p}$ on the lattice can then be associated with a unique basis point $\mathbf{p}_j$, and three unique integers l, m, and n, such that $\mathbf{p} = \mathbf{p}_j + l\mathbf{a}_1 + m\mathbf{a}_2 + n\mathbf{a}_3$. Here, j is referred to as the sub-lattice index, since it corresponds to points on the Bravais lattice formed by applying the primitive translation vectors to the point $\mathbf{p}_j$. In the case of the honeycomb lattice, the basis consists of two points $\mathbf{p}_0 = (0,0)$ and $\mathbf{p}_1 = (0, 1/\sqrt{3})$, and the primitive translation vectors are equal to the primitive vectors of the triangular lattice in eq. (2).
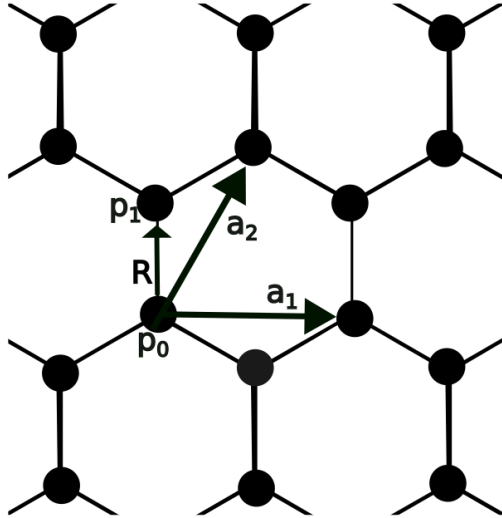
Figure 1: The figure shows the honeycomb lattice. Here, a_1 and a_2 are the primitive translation vectors of the lattice, R is the translation vector between the basis elements, and p_0 and p_1 are the two basis elements.

In the study of crystalline substances, the symmetries of the lattice are important to the properties of the substance. This is because physical properties are often invariant under symmetry operations. A symmetry operation is a transformation of the lattice that keeps angles and distances between points constant, and does not change the lattice. This means that a point that was a lattice point before the symmetry operation, remains a lattice point after the symmetry operation. An example of a symmetry operation for the triangular lattice is a rotation by 60° around a lattice point. A notable subset of the set of symmetry operations, is the point symmetry group, which is a group that consists of symmetry operations that leave a point in space fixed. Examples of possible point symmetry operations are rotations, inversions, and reflections. An important property of the point symmetry group is that it can be represented as a subset of the special orthogonal group. This means that every point symmetry operation can be represented as a linear transformation in Euclidean space.

3 The Heisenberg model

3.1 The Heisenberg Hamiltonian

The Heisenberg model is used to describe the behaviour of magnetic materials. In particular, it is used to describe materials where the electrons are strongly bonded to the atoms. In this case, the atoms bond with other atoms through the overlapping wave functions of the electrons in the valence shell of the atoms. Since the electrons are localized around an atom, the spins can be seen as localized at the atom itself. The that appears in the Heisenberg model is therefore the sum of the spins of the valence electrons of the atom. Due to Hund's rule, the valence electrons will occupy equal spin states until all of the equal spin states in the valence shell are occupied. If there are more valence electrons available, the opposite spin states will be filled with the remaining electrons, causing the total spin to decrease. Materials with atoms with small total spin, such as $S = 1/2$, will have strong quantum effects, while materials with larger total spin will behave closer to a classical system. When the spin orbital interaction is negligible, the spins only interact with other spins. This causes the spin space to be independent of the physical lattice space, allowing for three dimensional spin configurations on two dimensional lattices.

The Heisenberg model describes a material as a crystalline structure where each lattice point has a spin associated to it, and all the lattice points have spins of equal magnitude. The quantum Heisenberg Hamiltonian is given by the expression

$$\hat{H} = \frac{1}{2} \sum_i \sum_j J_{i,j} \hat{\mathbf{S}}(\mathbf{r}_i) \cdot \hat{\mathbf{S}}(\mathbf{r}_j) \tag{3}$$

where $J_{i,j}$ is the interaction energy between lattice points i and j, and $\hat{\mathbf{S}}(\mathbf{r}_i)$ is the spin operator corresponding to lattice point $\mathbf{r}_i$. When the spin of each atom is larger than $1/2$, it is possible to approximate the quantum Heisenberg model as a classical model as described above. In the classical Heisenberg model the spin operators become classical spin vectors which are allowed to have any configuration in three dimensions. The classical Heisenberg Hamiltonian is then given by the following expression:

$$H = \frac{1}{2} \sum_i \sum_j J_{i,j} \mathbf{S}(\mathbf{r}_i) \cdot \mathbf{S}(\mathbf{r}_j) \tag{4}$$

where $S(\mathbf{r}_i)$ is the classical spin vector corresponding to lattice point $\mathbf{r}_i$.

In order to simplify the Heisenberg model in eq. (4), we must make assumptions about the interaction energy $J_{i,j}$. A common way of simplifying the model, is to let $J_{i,j}$ only depend on the translation vector between the lattice points $\mathbf{r}_i$ and $\mathbf{r}_j$. This is a reasonable assumption since it is expected that the atoms interact in the same way when the surroundings are identical. Formally, this means that if there are lattice points at both $\mathbf{r}$ and $\mathbf{r} + \mathbf{u}$, the coupling between the spins at the lattice points only depends on $\mathbf{u}$. Using this, it is now possible to rewrite the Heisenberg Hamiltonian in the following way:

$$H = \frac{1}{2} \sum_i \sum_{\mathbf{u}} J(\mathbf{u}) \mathbf{S}(\mathbf{r}_i) \cdot \mathbf{S}(\mathbf{r}_i + \mathbf{u}) \tag{5}$$

It is also common to assume that $J(\mathbf{u})$ is invariant under operations from the point symmetry group of the lattice. This means that if T is a linear transformation that represents an element of the point symmetry group, we have that

$$J(\mathbf{u}) = J(T\mathbf{u}) \tag{6}$$

Using this, it is possible to categorize the translation vectors based on whether they are correlated through a point symmetry operation. Formally, we can consider the point symmetry group of the lattice $\mathcal{G}$ and the set of all translation vectors on the lattice U. A group action of $\mathcal{G}$ on U can then be defined by letting $g\mathbf{u} = T_g\mathbf{u}$, where $g \in \mathcal{G}$, $\mathbf{u} \in U$, and T_g is the representation of g as a linear transformation. We can then categorize U by considering the orbits of U under the action of $\mathcal{G}$, where the orbit of an element $\mathbf{u} \in U$ is the set of all translation vectors in U that can be obtained by acting with a point symmetry operation on $\mathbf{u}$. The orbit of $\mathbf{u} \in U$ can thus be written as

$$\text{Orb}(\mathbf{u}) = \{g\mathbf{u} \mid g \in \mathcal{G}\} \tag{7}$$

An equivalent construction would be to consider the equivalence relation $\sim$ on U defined by two vectors $\mathbf{u}, \mathbf{v} \in U$ being equivalent if $\mathbf{u} = T_g\mathbf{v}$ for some $g \in \mathcal{G}$. The equivalence classes of U under this relation, would then be equal to the orbits of U. It follows from the definition of equivalence classes that the orbits of U form a disjoint partition of U. Using this construction, we see that eq. (6) is equivalent to $J(\mathbf{u})$ only being dependent on the orbit of $\mathbf{u}$. It is therefore possible to assign an interaction energy to each orbit of U. If we consider the honeycomb lattice, a translation vector with minimum magnitude would be the translation vector between the two points in the basis. Since the point symmetry group of the honeycomb lattice include rotations by 60°, it follows that all of the translation vectors with minimum magnitude are
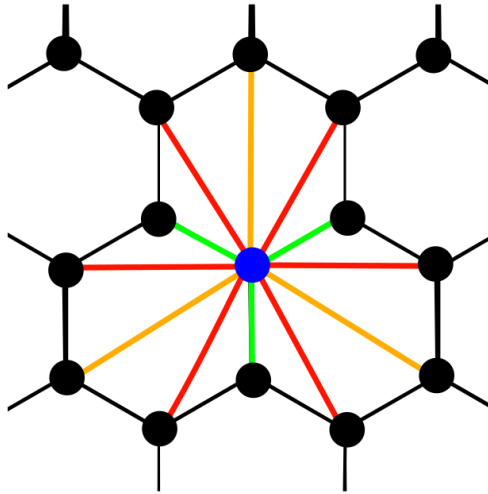
Figure 2: First (green), second (red), and third (orange) nearest neighbour couplings on the honeycomb lattice.

in the same orbit. This orbit containing all the translation vectors with minimum magnitude, represents the nearest neighbour interactions on the honeycomb lattice. Similarly if we consider the orbit of the primitive translation vector $\mathbf{a}_1$ in eq. (2), we see that the orbit contains all second nearest neighbour interactions on the honeycomb lattice. Figure 2 shows the first, second, and third neighbour interactions on the honeycomb lattice.

It is reasonable to assume that orbits representing longer range interactions will have significantly smaller contributions to the energy of the system then the orbits representing shorter range interactions. It is therefore common to only consider a small set of short range interactions in order to simplify the the system. A special case of this is the J_1-J_2 model, which only includes nearest and second nearest neighbour interactions. Here, all nearest neighbor interactions have an interaction energy of J_1, while all second nearest neighbour interactions have interaction energy J_2. The Hamiltonian then simplifies to

$$H = J_1 \sum_{\langle i,j \rangle} \mathbf{S}_i \cdot \mathbf{S}_j + J_2 \sum_{\langle \langle i,j \rangle \rangle} \mathbf{S}_i \cdot \mathbf{S}_j \tag{8}$$

where $\langle i, j \rangle$ denotes all nearest neighbour pairs and $\langle \langle i, j \rangle \rangle$ denotes all second nearest neighbour pairs.

10

4 Ground states of the Heisenberg Hamiltonian

4.1 Single and multi-q states

The ground states of the Heisenberg model are important because they largely govern the behaviour of the model at lower temperatures. While a general solution for the ground states of the Heisenberg Hamiltonian has never been found, several methods for finding ground states exist. One such method is to Fourier transform the spin and interaction energy in eq. (5):

$$H = \frac{1}{2} \sum_j \sum_{\mathbf{u}} J(\mathbf{u}) \mathbf{S}(\mathbf{r}_j) \cdot \mathbf{S}(\mathbf{r}_j + \mathbf{u}) \tag{9}$$

$$= \frac{1}{2N_p} \sum_j \sum_{\mathbf{u}} \sum_{\mathbf{q}} \sum_{\mathbf{q}'} \sum_{\mathbf{q}''} J(\mathbf{q}'') e^{i\mathbf{a} \cdot \mathbf{q}''} \mathbf{S}(\mathbf{q}) e^{i\mathbf{q} \cdot \mathbf{r}_j} \cdot \mathbf{S}(\mathbf{q}') e^{i\mathbf{q}' \cdot (\mathbf{r}_j + \mathbf{u})} \tag{10}$$

$$= \frac{1}{2N_p} \sum_j \sum_{\mathbf{u}} \sum_{\mathbf{q}} \sum_{\mathbf{q}'} \sum_{\mathbf{q}''} J(\mathbf{q}'') e^{i\mathbf{u} \cdot (\mathbf{q}'' + \mathbf{q}')} \mathbf{S}(\mathbf{q}) \cdot \mathbf{S}(\mathbf{q}') e^{i\mathbf{r}_j \cdot (\mathbf{q} + \mathbf{q}')} \tag{11}$$

$$= \frac{1}{2N_p} \sum_{\mathbf{q}} \sum_{\mathbf{q}'} \sum_{\mathbf{q}''} J(\mathbf{q}'') N_p \delta_{\mathbf{q}'', -\mathbf{q}'} \mathbf{S}(\mathbf{q}) \cdot \mathbf{S}(\mathbf{q}') N_p \delta_{\mathbf{q}, -\mathbf{q}'} \tag{12}$$

$$= \frac{N_p}{2} \sum_{\mathbf{q}} J(\mathbf{q}) \mathbf{S}(\mathbf{q}) \cdot \mathbf{S}(-\mathbf{q}) \tag{13}$$

where q, q', and q'' are wave numbers in Fourier space, N_p is the number of atoms, δ is the Kronecker delta, and

$$J(\mathbf{u}) = \sum_{\mathbf{q}} J(\mathbf{q}) e^{i\mathbf{q} \cdot \mathbf{u}} \tag{14}$$

$$\mathbf{S}(\mathbf{r}) = \frac{1}{\sqrt{N_p}} \sum_{\mathbf{q}} \mathbf{S}(\mathbf{q}) e^{i\mathbf{q} \cdot \mathbf{r}} \tag{15}$$

Single-q states then refer to states that only have a single Fourier mode in reciprocal space. The spin spiral states on the honeycomb lattice are examples of single-q states. They are given by the following expression:

$$\mathbf{S}(\mathbf{r}) = \hat{\mathbf{x}} \cos(\mathbf{q} \cdot \mathbf{r}) + \hat{\mathbf{y}} \sin(\mathbf{q} \cdot \mathbf{r}) \tag{16}$$

on one sublattice, and as

$$\mathbf{S}(\mathbf{r}) = \hat{\mathbf{x}} \cos(\mathbf{q} \cdot \mathbf{r} + \phi_{\mathbf{R}}) + \hat{\mathbf{y}} \sin(\mathbf{q} \cdot \mathbf{r} + \phi_{\mathbf{R}}) \tag{17}$$

on the other sublattice, where $\phi_{\mathbf{R}} = \mathbf{q} \cdot \mathbf{R}$ is the phase caused by the translation between sub lattices, and $\hat{\mathbf{x}}$ and $\hat{\mathbf{y}}$ are the unit vectors in the x and y direction, respectively..

From eq. (13) it follows that those single-q states that correspond to a $\mathbf{q}$ such that $J(\mathbf{q})$ is a global minimum, will be ground states of the Hamiltonian. The spin spiral states in eqs. (16) and (17) have been widely studied, but there also exists a large number of competing multi-q states consisting of multiple Fourier modes.

In the forthcoming, we will i) find several multi-q ground states of the honeycomb lattice in real space, and ii) will then find the entropy of the classical fluctuations around the ground states. Here, i) will be described in section 4.3, and ii) will be described in section 5.

4.2   Rewriting the Hamiltonian

In order to find candidate multi-q states on the honeycomb grid, a method for rewriting Heisenberg Hamiltonians described in Balla et. al. (2019) [3] will be applied. We start by considering the rewritten J_1-J_2 Heisenberg Hamiltonian, and then show that it is equivalent to the J_1-J_2 Heisenberg Hamiltonian in eq. (8). The rewritten Hamiltonian is given by the following expression:

$$H = \frac{J_2}{2} \sum_i \left(\left(\alpha \mathbf{S}(\mathbf{r}_i) + \sum_{\mathbf{u} \in \mathrm{Orb}(\mathbf{R})} \mathbf{S}(\mathbf{r}_i + \mathbf{u}) \right)^2 - \alpha^2 - Z \right) \tag{18}$$

where $\mathrm{Orb}(\mathbf{R})$ is the orbit containing the nearest neighbor translation vectors, α is a constant that can be used to adjust the ratio between J_1 and J_2, and Z is the number of nearest neighbours, which is equal to 4 in the case of the honeycomb lattice. By evaluating the square we see that each nearest neighbour and each second nearest neighbour interaction is represented by a term in each square. However, since we sum over all lattice points, each nearest neighbour interaction is counted twice, while each second nearest neighbour interaction is counted once. If we then let $\alpha = J_1/2J_2$ we obtain that eq. (18) is equivalent to eq. (8).

In general this method allows to sum over more orbits if it is of interest for the lattice and material in question. It is also possible to sum over different sections of
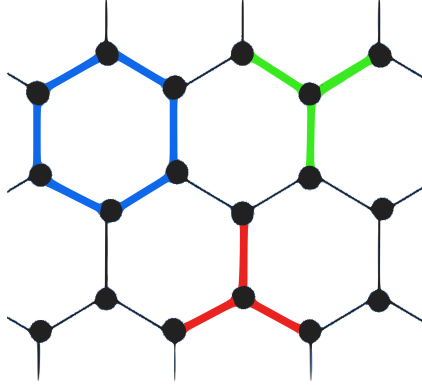
Figure 3: Blue outlines the hexagon shape which would be summed over in eq. (19). Green and red shows the two shapes that are summed over in eq. (18).

lattice points as long as the resulting square includes all the interactions in the orbits of interest. For example, it is possible to sum over the hexagons in the honeycomb lattice, shown in blue in fig. 3, to generate a model containing both first, second and third nearest neighbour couplings:

$$H = \sum_{\hexagon} \left(\mathbf{S}_1 + \mathbf{S}_2 + \mathbf{S}_3 + \mathbf{S}_4 + \mathbf{S}_5 + \mathbf{S}_6 \right)^2 - 6 \tag{19}$$

where the length of the spins have been assumed to be unity for simplicity. Here, S_1-S_6 refers to the spins in the hexagon, and the sum is over all the hexagons in the honeycomb lattice. This leads to a Heisenberg model with couplings $J_1 = 2J_2$ and $J_3 = J_2$. Here, J_3 is the coupling between the lattice points on opposite sides of the hexagon (see fig. 2), which are also the third nearest neighbour couplings on the honeycomb grid.

4.3   Ground states on the Honeycomb lattice

In order to find candidate multi-q states, we focus on the $J1 - J2$ model in eq. (18) with $\alpha = 1$, which means that $J_1 = 2J_2$. Writing out the terms in the equation results
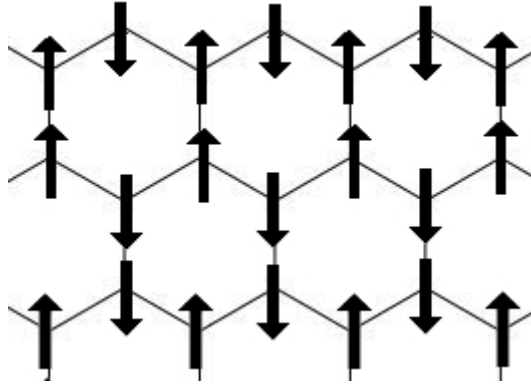
13

Figure 4: A co-linear ground state for $J_1 = 2J_2$. This state is a special case of the state in fig. 6 where $\theta = 0$, as well as a single-q spin spiral state where $q = \mathbf{b}_2/2$

in:

$$H = \frac{J_2}{2} \sum_i (\mathbf{S}_{i,0} + \mathbf{S}_{i,1} + \mathbf{S}_{i,2} + \mathbf{S}_{i,3})^2 - 4 \tag{20}$$

where it is summed over all the red and green shapes shown in fig. 3, and $\mathbf{S}_{i,0}$, $\mathbf{S}_{i,1}$, $\mathbf{S}_{i,2}$, and $\mathbf{S}_{i,3}$ are the four points in the shape surrounding lattice point i. It follows from eq. (20) that any state such that the spins in each shape sum to zero, is a ground state of the Hamiltonian. An example of such a ground state is the co-linear state shown in figure 7.

It is now possible to find ground states by first choosing four spin vectors which sum to zero, and then find a pattern where each lattice point has three neighbouring lattice points, each with one of the four chosen spin vectors. Figure 6 shows an example of such a pattern, where $\mathbf{a}$, $\mathbf{b}$, $\mathbf{c}$, and $\mathbf{d}$ are four vectors such that $\mathbf{a} + \mathbf{b} + \mathbf{c} + \mathbf{d} = 0$. The box in the figure shows the periodicity of the state by outlining a periodic cell.

For each such pattern, we can now find a parameterized set of ground states by applying a parameterized set of four vectors of equal length that sum to 0. In a plane, four vectors summing to zero will always form a parallelogram. In three dimensions this can be generalized by letting half of the parallelogram rotate freely around the axis formed by the diagonal of the parallelogram as shown in fig. 5. We let θ be the angle between $\mathbf{a}$ and the z-axis, while ϕ is the angle by which $\mathbf{c}$ and $\mathbf{d}$ have been rotated around the z-axis. For $\phi = 0$ we get that $\mathbf{c} = -\mathbf{a}$ and $\mathbf{d} = -\mathbf{b}$. This gives
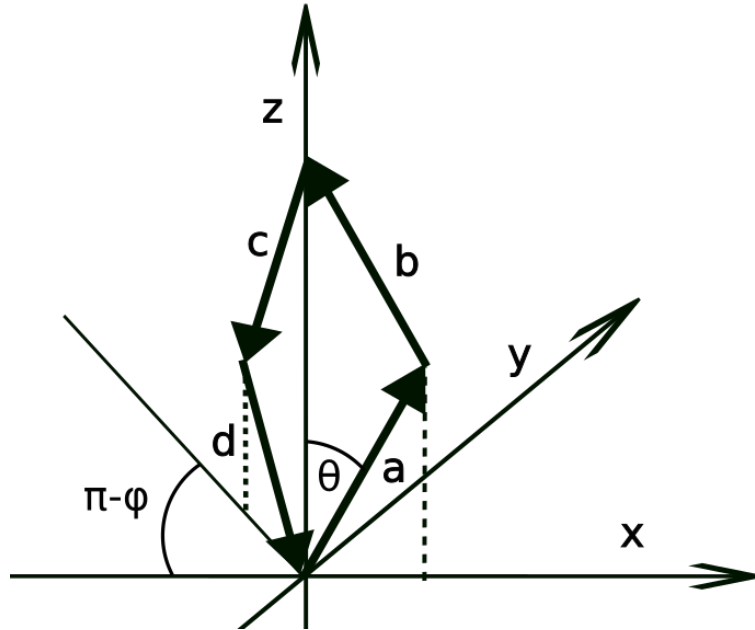
Figure 5: The four vectors in the parameterization. The vectors **a** and **b** are fixed in the xz-plane while the vectors **c** and **d** are equal to $-$**a** and $-$**b** rotated by ϕ around the z-axis.

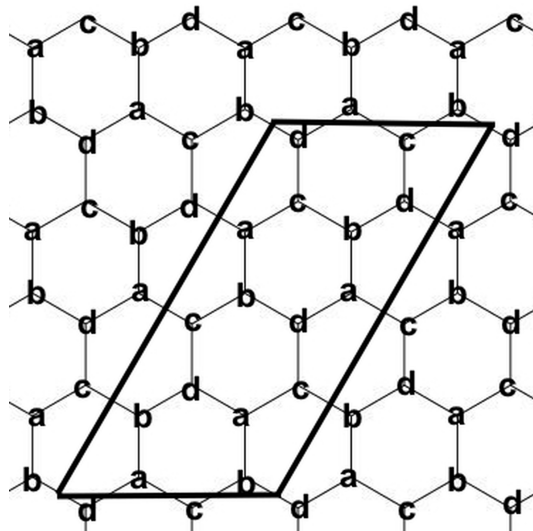Figure 6: A ground state for $J_1 = 2J_2$. The black box outlines the periodic cell of the state.

the following parameterization:

$$\mathbf{a} = (\sin\theta, 0, \cos\theta)$$
$$\mathbf{b} = (-\sin\theta, 0, \cos\theta)$$
$$\mathbf{c} = (\cos\phi\sin\theta, \sin\phi\sin\theta, -\cos\theta) \tag{21}$$
$$\mathbf{d} = (-\cos\phi\sin\theta, -\sin\phi\sin\theta, -\cos\theta)$$

where $\theta \in [0, \pi]$, and $\phi \in [0, \pi]$. It follows that the state in fig. 6 is a ground state for all values of θ and ϕ. We see that when $\theta = 0$, the state in fig. 6 is equal to the state in fig. 7, and when $\theta = \pi/2$ the state in fig. 6 is a coplanar state.

The pattern in fig. 6 is just an example of a pattern that gives a set of parameterized ground states. If we disregard periodicity in the $\mathbf{a}_2$ direction, it is possible to create an infinite number of such patterns. In order to construct these patterns, we start by pairing $\mathbf{a}$, $\mathbf{b}$, $\mathbf{c}$, and $\mathbf{d}$ into two pairs P_1 and P_2, such that $P_1 = \{\mathbf{a}, \mathbf{b}\}$ and $P_2 = \{\mathbf{c}, \mathbf{d}\}$. We then require that $\mathbf{S}(\mathbf{r}) = \mathbf{S}(\mathbf{r} + 2\mathbf{a}_1)$, that $\mathbf{S}(\mathbf{r}) \neq \mathbf{S}(\mathbf{r} + \mathbf{a}_1)$ (unless $\mathbf{a} = \mathbf{b}$), and that $\mathbf{S}(\mathbf{r})$ is in the same pair as $\mathbf{S}(\mathbf{r}+\mathbf{a}_1)$. Furthermore, it is also required that if a point $\mathbf{r}$ is in sublattice 0, meaning the point is in the same sublattice as p_0 in fig. 1, then $\mathbf{S}(\mathbf{r} + \mathbf{R}) = \mathbf{S}(\mathbf{r} + \mathbf{a}_1)$. The last requirement is that $\mathbf{S}(\mathbf{r})$ and $\mathbf{S}(\mathbf{r} + \mathbf{a}_2)$ must be in different pairs. We note that the pattern in fig. 6 fulfills all of the above requirements.

Starting from the basis point $\mathbf{p}_0$, it is now possible to create a new pattern by choosing a vector from P_2, and then continuing to assign vectors to $p_0 + n\mathbf{a}_2$, following the rule that you must assign a vector from P_1 if n is odd, and P_2 if n is even. The spins on the other lattice points, are uniquely defined through the above requirements. This is true because translating by $\mathbf{a}_1$ is equivalent to alternating the vectors in the same pair, while the spins in the other sublattice are given by $\mathbf{S}(\mathbf{r} + \mathbf{R}) = \mathbf{S}(\mathbf{r} + \mathbf{a}_1)$. From this it follows that for every lattice point along the $\mathbf{p}_0 + n\mathbf{a}_1$ line, we can choose between two different vectors, where every choice leads to a different pattern. On a finite lattice with N_U number of points along the $\mathbf{p}_0 + n\mathbf{a}_1$ line, obtain that the number of patterns that can be constructed with the above construction is 2^{N_U}.

For each of these patterns there exists a parameterized set of ground states unique to the pattern. While some ground states might overlap between the patterns or with the set of spin spiral states, the ground states are unique multi-q states for the majority of the values of ϕ and θ. The pattern in fig. 6 includes double-q states,

16

meaning that there are two Fourier modes contributing to the state. We see that the contributing reciprocal vectors $\mathbf{q}$ within the first Brillouin zone are $\mathbf{Q}$, $-\mathbf{Q}$, and $2\mathbf{Q}$, where $\mathbf{Q} = \mathbf{b}_1/2 + 3\mathbf{b}_2/4$. Here, $\mathbf{b}_1 = 2\pi(1, -1/\sqrt{3})$ and $\mathbf{b}_2 = 2\pi(0, 2/\sqrt{3})$ are the reciprocal basis vectors of the honeycomb lattice, which are defined by the property $\mathbf{a}_i \cdot \mathbf{b}_j = 2\pi\delta_{i,j}$. By choosing patterns with longer periodicity in the $\mathbf{a}_2$ direction, it is possible to create ground states with an arbitrary number of contributing Fourier modes.

5 Order by disorder

5.1 Calculation of the ground state entropy

At low and finite temperatures, the system will favour ground states with higher entropy. This means that ground states with a large number of low energy states surrounding them will have a larger probability of being realized at low, but finite temperatures. The ground state in fig. 6 is equal to one of the single-q ground states favoured by quantum fluctuations when $\theta = 0$ [7]. This makes the state in fig. 6 a good candidate for the entropy calculation as it becomes possible to compare the entropy of the multi-q states with the single-q spin spiral states. We will therefore focus on the ground state in fig. 6.

In the quantum case, the Holstein-Primakoff transformation would be used to find the contribution of the quantum fluctuations to the ground state energy by perturbing the spin operators with bosonic creation and annihilation operators [4]. In the classical case however, a similar analysis can be done by perturbing the spins of the classical spin vectors, and taking the integral over the perturbations. The perturbations of the spins must be in directions orthogonal to the spin vector of each spin. In order to facilitate this calculation, we start by introducing the rotated spin vectors $\mathbf{S}'_i$, which are rotated in such a way that they always point in the z-direction:

$$\mathbf{S}_i = T_i \mathbf{S}'_i \tag{22}$$

where $\mathbf{S}_i$ is the spin vector at lattice point i, $\mathbf{S}'_i = (0, 0, 1)$, and T_i is the rotation matrix corresponding to lattice point i. We perturb the spins around the ground state by adding perturbations to the x and y component of $\mathbf{S}'_i$:

$$\mathbf{S}'_i = (x_i, y_i, \sqrt{1 - x_i^2 - y_i^2})$$

where x_i and y_i are small perturbations to the spin $\mathbf{S}'_i$. At low temperatures, only small perturbations will contribute. We can therefore Taylor expand the z-component to second order. This gives

$$\mathbf{S}'_i \approx (x_i, y_i, 1 - \frac{1}{2}(x_i^2 + y_i^2)) \tag{23}$$

In order to find the Hamiltonian as a function of the perturbations x_i and y_i, the dot product between two spins is calculated:

$$\mathbf{S}_i \cdot \mathbf{S}_j = \mathbf{S}'_i T_i^T T_j \mathbf{S}'_j \tag{24}$$

18

When substituting equation (23) into equation (24), we only keep terms up to quadratic order, which is consistent with the approximation in equation (23). Since the ground state only has 4 possible spin directions, there are only 4 possible rotation matrices:

$$T_a = \begin{bmatrix} \cos\theta & 0 & \sin\theta \\ 0 & 1 & 0 \\ -\sin\theta & 0 & \cos\theta \end{bmatrix} \quad T_b = \begin{bmatrix} \cos\theta & 0 & -\sin\theta \\ 0 & 1 & 0 \\ \sin\theta & 0 & \cos\theta \end{bmatrix} \quad (25)$$

$$T_c = \begin{bmatrix} -\cos\theta\cos\phi & -\sin\phi & \cos\phi\sin\theta \\ -\cos\theta\sin\phi & \cos\phi & \sin\phi\sin\theta \\ -\sin\theta & 0 & -\cos\theta \end{bmatrix} \quad T_d = \begin{bmatrix} -\cos\theta\cos\phi & -\sin\phi & -\cos\phi\sin\theta \\ -\cos\theta\sin\phi & \cos\phi & -\sin\phi\sin\theta \\ \sin\theta & 0 & -\cos\theta \end{bmatrix}$$

where T_a, T_b, T_c, and T_d denotes the rotation matrices corresponding to the spins who have spin vector $\mathbf{a}$, $\mathbf{b}$, $\mathbf{c}$, or $\mathbf{d}$, respectively.

We now take advantage of the periodicity of the ground state to divide the lattice into periodic cells shown in figure 7. Each spin $\mathbf{S}_{j,l,m,n,\delta}$ can be represented by 5 indices, where the two first indices j and l give the position of the periodic cell along the $\mathbf{a}_1$ and $\mathbf{a}_2$ axis respectively. The next two indices m and n, show the position of the spin within the periodic cell, and δ is the sub-lattice index. The indices m and n are defined such that the bottom left lattice point in each periodic cell has indices $m = 0$ and $n = 0$, and m increases along the $\mathbf{a}_1$ axis, while n increases along the $\mathbf{a}_2$ axis.

By applying periodic boundary conditions, the Hamiltonian can now by rewritten as a sum over the periodic cells. Here, each term includes all internal interactions as well as the interactions between the respective periodic cell and half of it's neighbouring periodic cells. In this way, all interactions are accounted for when all periodic cells are summed over. Figure 7 shows which periodic cells interact in each term. The term in the Hamiltonian representing the indices of the middle cell will include the interactions with the cells surrounded by blue, but will not include interactions with the cells surrounded by red. Appendix A has the Hamiltonian written out in full.
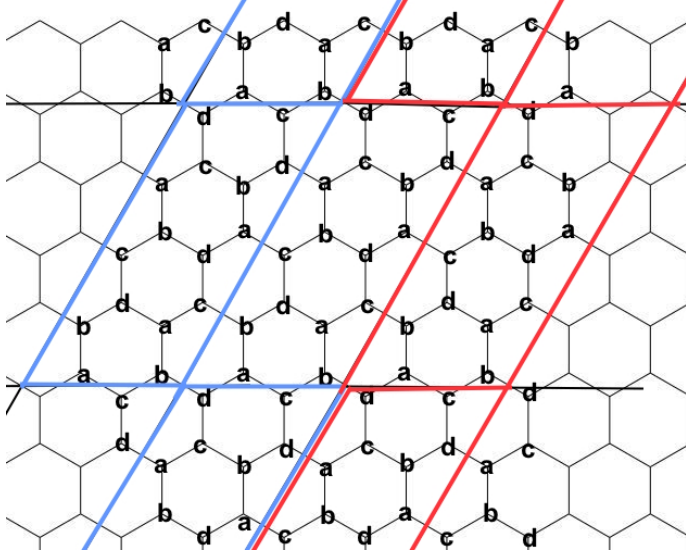
Figure 7: The term in the Hamiltonian representing the indices (j, k) will count the interactions with the cells surrounded by blue, and will not include interactions with the cells surrounded by red.

We can now Fourier transform with respect to j and l. This yields:

$$x_{j,l,m,n,\delta} = \frac{1}{\sqrt{MN}} \sum_{k_1} \sum_{k_2} x_{k_1,k_2,m,n,\delta} e^{2\pi i \left(\frac{jk_1}{M} + \frac{lk_2}{N} \right)} \tag{26}$$

where M and N are the number of periodic cells along the $\mathbf{a}_1$ and $\mathbf{a}_2$ axes respectively. The Fourier transform causes all terms linear of x and y in the Hamiltonian to cancel. This needs to be since the existence of linear terms in the Hamiltonian implies that there are perturbations with lower energy than the state we are perturbing around. This leaves only quadratic and constant terms. The quadratic terms are then Fourier transformed in the following way.

$$\sum_{\mathbf{j}} x_{\mathbf{j}} y_{\mathbf{j}+\mathbf{v}} = \frac{1}{MN} \sum_{\mathbf{j}} \sum_{\mathbf{k}} \sum_{\mathbf{k}'} x_{\mathbf{k}} y_{\mathbf{k}'} e^{i\mathbf{j}\cdot\mathbf{k}} e^{i(\mathbf{j}+\mathbf{v})\cdot\mathbf{k}'} \tag{27}$$

$$= \frac{1}{MN} \sum_{\mathbf{k}} \sum_{\mathbf{k}'} x_{\mathbf{k}} y_{\mathbf{k}'} MN \delta_{(\mathbf{k}+\mathbf{k}',0)} e^{i\mathbf{v}\cdot\mathbf{k}'} \tag{28}$$

$$= \frac{1}{2} \sum_{\mathbf{k}} \left(x_{\mathbf{k}} y_{-\mathbf{k}} e^{-i\mathbf{v}\cdot\mathbf{k}} + x_{-\mathbf{k}} y_{\mathbf{k}} e^{i\mathbf{v}\cdot\mathbf{k}} \right) \tag{29}$$

where $\mathbf{j} = (j, l)$ is a vector containing the indices of the periodic cell, $\mathbf{v}$ is a vector translating from one periodic cell to a neighbouring periodic cell, and $\mathbf{k} = 2\pi(\frac{k_1}{M}, \frac{k_2}{N})$.

20

Since $x_{\mathbf{j}} \in \mathbb{R}$, we know that $x_{\mathbf{k}} = x^*_{-\mathbf{k}}$. Since only quadratic terms remain, the Hamiltonian can be written in the following way:

$$H = -16MNJ_1 - \frac{1}{2}\sum_{\mathbf{k}} \mathbf{x}^{*T}_{\mathbf{k}} A_{\mathbf{k}} \mathbf{x}_{\mathbf{k}} \tag{30}$$

where $A_{\mathbf{k}}$ is a hermitian 32×32 matrix and $\mathbf{x}_{\mathbf{k}}$ is a vector containing all the $x_{\mathbf{k},m,n,\delta}$ and $y_{\mathbf{k},m,n,\delta}$ with the same $\mathbf{k}$. The free energy is independent of the ordering in $\mathbf{x}_k$ since any reordering will cause an equal reordering in the columns and rows of $A_{\mathbf{k}}$. Moving a row or a column of a matrix can only cause a sign change in the determinant, but since both the columns and rows are moved in the same way, any sign change will cancel out. In the calculations the $i+1$-th element of $x_{\mathbf{k}}$ is given by the following expression:

$$i = 16X + 8m + 2n + \delta \tag{31}$$

where X is one for $x_{\mathbf{k},m,n,\delta}$ and zero for $y_{\mathbf{k},m,n,\delta}$. Since there are 16 lattice points in each grid cell, $\mathbf{x}_{\mathbf{k}} \in \mathbb{C}^{32}$. We can now calculate the partition function Z.

$$Z = \int D\mathbf{x}\, e^{-\beta H} \tag{32}$$

$$= e^{16MNJ_1\beta} \int D\mathbf{x} \exp\left(-\frac{\beta}{2}\sum_{\mathbf{k}} \mathbf{x}^{*T}_{\mathbf{k}} A_{\mathbf{k}} \mathbf{x}_{\mathbf{k}}\right) \tag{33}$$

$$= e^{16MNJ_1\beta} \prod_{\mathbf{k}} \left(\frac{1}{\beta^{32}\det(A_{\mathbf{k}}/2\pi)}\right) \tag{34}$$

where $D\mathbf{x} = \prod_{\mathbf{k}} d\mathbf{x}_{\mathbf{k}}$, $\beta = 1/(k_B T)$, and we have used that

$$\int D\mathbf{x} \exp\left(-\frac{1}{2}\mathbf{x}^{*T} A\mathbf{x}\right) = \sqrt{\frac{1}{\det(A/2\pi)}} \tag{35}$$

We can then calculate the free energy per site f, using that

$$Z = \exp(-16\beta MNf) \tag{36}$$

The free energy per site then becomes:

$$f = -J1 + \frac{1}{16\beta MN}\sum_{\mathbf{k}} \left(\ln\left(\det(A_{\mathbf{k}}/2\pi)\right) + \ln\left(\beta^{32}\right)\right) \tag{37}$$

Applying units such that the Boltzmann's constant $k_B = 1$, the entropy per site s becomes

$$s = -\frac{\partial f}{\partial T} = -\frac{1}{16MN}\sum_{\mathbf{k}} \left(\ln\left(\det(A_{\mathbf{k}}/2\pi)\right) + \ln(T^{32}) - 32\right) \tag{38}$$

21

In order to find an analytical expression for $A_{\mathbf{k}}$, the symbolic programming language SageMath was used to find the expression for the Hamiltonian in real space. The Fourier transform and extraction of the matrix coefficients of $A_{\mathbf{k}}$ posed a technical challenge since, to the best of the authors knowledge, no such Fourier transform is intricit in any of the available symbolic programming languages such as eg. SageMath, Maple, Mathematica and SymPy. To overcome this problem, a python program was written in order to conduct these symbolic computations. Appendix A provides further details of the calculation.

5.2   Singularities in the free energy

When calculating the free energy, we need the determinant of $A_{\mathbf{k}}$ to be positive, but for certain values of $\mathbf{k}$, we get that $\det(A_{\mathbf{k}}) = 0$. Such values of $\mathbf{k}$ will be referred to as singularities since they cause the entropy to become infinite. Singularities of this form are well known, and also appear in the case of spin spirals. In this case, the solution is to subtract a reference entropy from the calculated entropy such that the zeros in the determinant cancel out. The idea behind this, is to assume that every ground state has the same set of perturbations that causes the entropy to go to infinity. Subtracting a reference entropy will then cause only the entropy that corresponds to the excitations of that ground state to remain. Mathematically, this means that if ξ is a parameter of a parameterized set of ground states, and the Hamiltonian of the perturbed states can be written as $H = C - \sum_{\mathbf{k}} \mathbf{x}_{\mathbf{k}}^T B_{\mathbf{k}}(\xi)\mathbf{x}_{\mathbf{k}}/2$ for some constant C, and matrix $B_{\mathbf{k}}(\xi)$, we can study the quantity

$$S(\xi) - S(\xi_0) = \sum_{\mathbf{k}} S_{\mathbf{k}}(\xi) - S_{\mathbf{k}}(\xi_0) \tag{39}$$

$$= \sum_{\mathbf{k}} \ln\left(\frac{\det(B_{\mathbf{k}}(\xi_0))}{\det(B_{\mathbf{k}}(\xi))}\right) \tag{40}$$

where $S(\xi)$ is the entropy of the ground state, $S_{\mathbf{k}}(\xi)$ is the entropy contribution from the perturbation mode $\mathbf{k}$, and ξ_0 is a reference ground state. If the singularities are the same in all the ground states, they will cancel in eq. (40). The difference in entropy between the ground states and the reference state can then be used to find the favoured ground states among the tested ground states.

For the present work, this method cannot be applied because the singularities are not the same in every ground state. The numerical results show that there is a clear difference between coplanar and non-coplanar states. The singularities of coplanar states form two lines through $\mathbf{k}$-space. These lines are defined through $k_1 = 0$, and

$k_2 = 2k_1$, respectively. In the case of non-coplanar states however, only the perturbation modes $\mathbf{k}$ on the line $k_1 = 0$ are singularities. This means that it is impossible to remove all singularities by subtracting a reference entropy.

The singularities have a physical interpretation as they represent perturbations to the ground state that do not change the energy of the system. For the calculation above, this means that there exists some $\mathbf{x_k} \neq 0$ such that $A_\mathbf{k}\mathbf{x_k} = 0$. The simplest example of this is a global rotation of all spins, which in the calculation above, refers to the case where $\mathbf{k} = 0$ and all the entries of $\mathbf{x_k}$ are equal. Another example for coplanar states, that arise when $\theta = \pi/2$, is any equal rotation of $\mathbf{a}$ and $\mathbf{c}$. This can be seen from the fact that $\mathbf{a}$ and $\mathbf{c}$ are parallel vectors in the case of a coplanar state. This means that if $\mathbf{a}$ and $\mathbf{c}$ are rotated equally, they will still remain parallel, and therefore sum to zero.

While the $\mathbf{k}$-modes that have singularities do not change within the non-coplanar and coplanar states, the multiplicities of the zero-eigenvalues do change. This means that there are values of ϕ and θ where $A_\mathbf{k}(\phi, \theta)$ has fewer zero-eigenvalues than other values of ϕ and θ for some $\mathbf{k}$-mode. Since $A_\mathbf{k}$ is hermitian, and therefore diagonalizable, the dimension of the eigenspace of a given eigenvalue must be equal to the multiplicity of that eigenvalue. The fact that the multiplicity of the zero-eigenvalue varies for different coplanar states, implies that there are more perturbations for some coplanar states that do not change the energy of the system. This poses the question whether the eigenvalues which are only zero for some, but not all choices of ϕ and θ, are important for the physics of the system. In order to study this, we note that $A_\mathbf{k}(\phi, \theta)$ is a continuous function of ϕ and θ. This implies that the eigenvalues $\lambda_i(\theta, \phi)$ of $A_\mathbf{k}(\theta, \phi)$ are also continuous functions of ϕ and θ.

If there exists an eigenvalue λ_i of $A_\mathbf{k}$ such that $\lambda_i(\phi_0, \theta_0) = 0$, and $\lambda_i(\phi_1, \theta_1) \neq 0$ for some ϕ_0, θ_0, ϕ_1, and θ_1, there must be choices of ϕ and θ such that λ_i is arbitrarily close to 0. The eigenvector corresponding to λ_i will then represent a low energy excitation around the ground state. In general, the area of ground states surrounding a ground state with a larger number of zero eigenvalues, will have ground states with a larger number of low energy excitations, leading to an increased entropy of the ground states. The entropy of the parameterized ground states must therefore increase as the ground state with the highest number of zero-eigenvalues is approached. As the entropy increases, so does the probability of the ground states being realized at low temperatures, which implies that the probability of a ground state being realized at

low temperatures increases as you approach ground states with higher numbers of zero eigenvalues.

In the numerical evaluation of the entropy, the determinant of $A_{\mathbf{k}}$ is assumed to be zero if the eigenvalues of $A_{\mathbf{k}}$ are approximately the same magnitude as the machine precision. More specifically, a limit of 10^{-15} was set, where if the eigenvalue was lower it is assumed to be zero. Figure 8 shows the number of zero eigenvalues as a function of ϕ and θ. We see that the ground state at $\theta = 0$ has the most zero eigenvalues, while the ground states at $\theta = \pi/2$ have the second most zero eigenvalues. When $\theta = 0$, $\mathbf{a}$ and $\mathbf{b}$ will point in the z-direction, while $\mathbf{c}$ and $\mathbf{d}$ will point in the opposite direction. The line of $\theta = 0$ in the plot therefore only represents a single colinear state. When $\theta = \pi/2$, the ground states are coplanar in the xy-plane, and the point defined by $\theta = \pi/2$ and $\phi = 0$, is a colinear state along the x-axis. The state $\theta = 0$ is a spin spiral state with $\mathbf{q} = \mathbf{b}_2/2$, and is shown in fig. 7. The favoured ground states among the parameterized set of ground states in fig. 6 are therefore the same as the favoured spin spiral ground states found by Mulder et. al. (2010) [7], where it was shown that the colinear spin spiral ground states were those favoured by quantum fluctuations on the honeycomb J_1-J_2 Heisenberg model in the case where $J_1 = 2J_2$. It should be noted that this comparison is physically reasonable only in the case where the system can be approximated classically, i.e., for systems with larger spins.
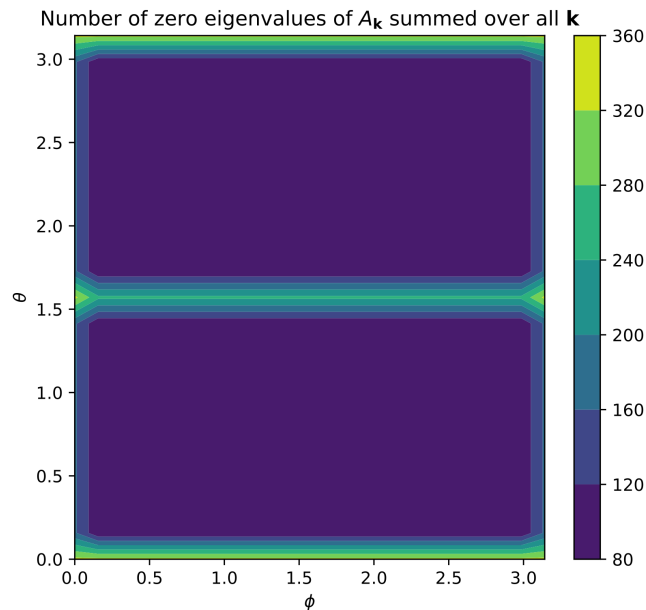
Figure 8: The figure shows the total number of zero eigenvalues of $A_{\mathbf{k}}$ summed over all $\mathbf{k}$ for each value of ϕ and θ

6 Summary and conclusion

In the present work, new multi-q ground states of the honeycomb J_1-J_2 Heisenberg model were investigated. The aim of this investigation was to see whether these new multi-q ground states are competitive with the favoured spin spiral ground states described in Mulder et al. (2010)[7] in a low temperature environment. This was achieved by utilizing a method developed by Balla. et. al. (2019) [3] to rewrite the Hamiltonian in a way that allows for a geometric interpretation of the ground states of the J_1-J_2 honeycomb Heisenberg model. This way, multiple parameterized sets of new ground states were found.

Specifically, the Heisenberg Hamiltonian was rewritten to prove that if the sum of a spin and its three nearest neighbors is zero for all spins, then the resulting configuration must be a ground state of the J_1-J_2 Heisenberg model in the case where $J_1 = 2J_2$. A method was then developed to construct a large number of such ground states through the use of a parameterized set of four vectors that sum to zero. In order to find which states are favoured by the system at low, but finite temperatures,

25

a set of parameterized ground states, which includes one of the favoured ground states of the spin spiral ground states, was investigated.

The entropy of the chosen set of ground states was then found by computing the partition function of small perturbations of the ground states. Here, it was found that there exists perturbations that do not change the energy of the perturbed state, which causes the entropy to become infinite. For spin spirals, it is possible to remove such singularities by subtracting a reference entropy. For the present ground states however, this is not possible because both the **k**-modes with singularities and the number of zero-eigenvalues of $A_{\mathbf{k}}$ change for different values of the angles ϕ and θ. Due to the continuity of the eigenvalues in ϕ and θ, the ground states in the region surrounding a ground state with a higher number of zero eigenvalues, must have a higher number of low energy excitations, which leads to a higher entropy of the surrounding ground states. The number of zero eigenvalues of a ground state is thus indicative of the amount of low energy excitations around the ground state. This means that ground states with more zero eigenvalues have a higher probability of being realized in a low temperature environment.

The numerical evaluation of the eigenvalues of $A_{\mathbf{k}}$ reveals that: i) Coplanar states are more likely of being realized at low temperatures than non-coplanar states, and ii) among the coplanar states, the colinear states have the highest probability of being realized at low temperatures. The aim of this investigation was to see whether the new obtained multi-q ground states are competitive with the favoured spin spiral ground states described in Mulder et al. (2010)[7] in a low temperature environment. The colinear states favoured in our investigation are the same states as the favoured states found by Mulder et al. (2010) for the case $J_1 = 2J_2$. This leads to the conclusion that the honeycomb Heisenberg model with $J_1 = 2J_2$ favours colinear states at low temperatures.

References

[1] P. W. ANDERSON. The resonating valence bond state in la2cuo4 and super-conductivity. *Science (American Association for the Advancement of Science)*, 235(4793):1196–1198, 1987.

[2] L. Balents. Spin liquids in frustrated magnets. *Nature*, 464(7286):199–208, 2010.

[3] P. Balla, Y. Iqbal, and K. Penc. Affine lattice construction of spiral surfaces in frustrated heisenberg models. *Physical review. B*, 100(14), 2019.

[4] T. Holstein and H. Primakoff. Field dependence of the intrinsic domain magne-tization of a ferromagnet. *Physical review*, 58(12):1098–1113, 1940.

[5] D. Litvin. The luttinger-tisza method. *Physica*, 77(2):205–219, 1974.

[6] J. Luttinger and L. Tisza. Theory of dipole interaction in crystals. *Physical review*, 70(11-12):954–964, 1946.

[7] A. Mulder, R. Ganesh, L. Capriotti, and A. Paramekanti. Spiral order by disor-der and lattice nematic order in a frustrated heisenberg antiferromagnet on the honeycomb lattice. *Physical review. B, Condensed matter and materials physics*, 81(21), 2010.

[8] T. Okubo, S. Chung, and H. Kawamura. Multiple-q states and the skyrmion lattice of the triangular-lattice heisenberg antiferromagnet under magnetic fields. *Physical review letters*, 108(1):017206–017206, 2012.

[9] T. Shimokawa, T. Okubo, and H. Kawamura. Multiple-q states of the j1-j2 classical honeycomb-lattice heisenberg antiferromagnet under a magnetic field. *Physical review. B*, 100(22), 2019.

[10] O. Smirnova, M. Azuma, N. Kumada, Y. Kusano, M. Matsuda, Y. Shimakawa, T. Takei, Y. Yonesaki, and N. Kinomura. Synthesis, crystal structure, and mag-netic properties of bi3mn4o12(no3) oxynitrate comprising s = 3/2 honeycomb lattice. *Journal of the American Chemical Society*, 131(23):8313–8317, 2009.

[11] T. Yildirim. Origin of the 150-k anomaly in lafeaso: competing antiferromag-netic interactions, frustration, and a structural phase transition. *Physical review letters*, 101(5):057010–057010, 2008.

A   Spin wave calculation

Taking all interactions into account, the full Hamiltonian becomes

$$\frac{H}{16MN} = J1 \sum_j \sum_k (\mathbf{S}_{j,k,0,0,0} \cdot (\mathbf{S}_{j,k,0,0,1} + \mathbf{S}_{j,k-1,1,3,1} + \mathbf{S}_{j,k-1,0,3,1})+$$

$$\mathbf{S}_{j,k,1,0,0} \cdot (\mathbf{S}_{j,k,1,0,1} + \mathbf{S}_{j,k-1,1,3,1}) + \mathbf{S}_{j,k,0,0,1} \cdot (\mathbf{S}_{j,k,0,1,0} + \mathbf{S}_{j-1,k,1,1,0})+$$

$$\mathbf{S}_{j,k,1,0,1} \cdot (\mathbf{S}_{j,k,0,1,0} + \mathbf{S}_{j,k,1,1,0}) + \mathbf{S}_{j,k,0,1,0} \cdot \mathbf{S}_{j,k,0,1,1} + \mathbf{S}_{j,k,1,1,0} \cdot \mathbf{S}_{j,k,1,1,1}+$$

$$\mathbf{S}_{j,k,0,1,1} \cdot (\mathbf{S}_{j-1,k,1,2,0} + \mathbf{S}_{j,k,0,2,0}) + \mathbf{S}_{j,k,1,1,1} \cdot (\mathbf{S}_{j,k,0,2,0} + \mathbf{S}_{j,k,1,2,0})+$$

$$\mathbf{S}_{j,k,0,2,0} \cdot \mathbf{S}_{j,k,0,2,1} + \mathbf{S}_{j,k,1,2,0} \cdot \mathbf{S}_{j,k,1,2,1} + \mathbf{S}_{j,k,0,2,1} \cdot (\mathbf{S}_{j-1,k,1,3,0} + \mathbf{S}_{j,k,0,3,0})+$$

$$\mathbf{S}_{j,k,1,2,1} \cdot (\mathbf{S}_{j,k,0,3,0} + \mathbf{S}_{j,k,1,3,0})) + \mathbf{S}_{j,k,0,3,0} \cdot \mathbf{S}_{j,k,0,3,1}+$$

$$\mathbf{S}_{j,k,1,3,0} \cdot \mathbf{S}_{j,k,1,3,1} + \mathbf{S}_{j,k,0,3,1} \cdot \mathbf{S}_{j-1,k+1,1,0,0})+$$

$$J2 \sum_j \sum_k \sum_\delta (\mathbf{S}_{j,k,0,0,\delta} \cdot (\mathbf{S}_{j,k-1,0,3,\delta} + \mathbf{S}_{j,k-1,1,3,\delta}+$$

$$\mathbf{S}_{j,k,1,0,\delta} + \mathbf{S}_{j,k,0,1,\delta} + \mathbf{S}_{j-1,k,1,1,\delta} + \mathbf{S}_{j-1,k,1,0,\delta})+$$

$$\mathbf{S}_{j,k,1,0,\delta} \cdot (\mathbf{S}_{j,k-1,1,3,\delta} + \mathbf{S}_{j,k,1,1,\delta} + \mathbf{S}_{j,k,0,1,\delta})+$$

$$\mathbf{S}_{j,k,0,1,\delta} \cdot (\mathbf{S}_{j,k,1,1,\delta} + \mathbf{S}_{j,k,0,2,\delta} + \mathbf{S}_{j-1,k,1,2,\delta} + \mathbf{S}_{j-1,k,1,1,\delta})+$$

$$\mathbf{S}_{j,k,1,1,\delta} \cdot (\mathbf{S}_{j,k,0,2,\delta} + \mathbf{S}_{j,k,1,2,\delta})+$$

$$\mathbf{S}_{j,k,0,2,\delta} \cdot (\mathbf{S}_{j,k,1,2,\delta} + \mathbf{S}_{j,k,0,3,\delta} + \mathbf{S}_{j-1,k,1,3,\delta} + \mathbf{S}_{j-1,k,1,2,\delta})+$$

$$\mathbf{S}_{j,k,1,2,\delta} \cdot (\mathbf{S}_{j,k,0,3,\delta} + \mathbf{S}_{j,k,1,3,\delta})+$$

$$\mathbf{S}_{j,k,0,3,\delta} \cdot (\mathbf{S}_{j,k,1,3,\delta} + \mathbf{S}_{j-1,k+1,1,0,\delta} + \mathbf{S}_{j-1,k,1,3,\delta}))$$

The dot products are only calculated up to quadratic order. There are 6 possible outcomes of the dot product. If $\mathbf{S}_1 = \mathbf{a}$ and $\mathbf{S}_2 = \mathbf{b}$, the dot product becomes:

$$\mathbf{S}_1 \cdot \mathbf{S}_2 = -\frac{1}{2} x_1^2 \cos(\theta)^2 + x_1 x_2 \cos(\theta)^2 - \frac{1}{2} x_2^2 \cos(\theta)^2 - \frac{1}{2} y_1^2 \cos(\theta)^2 -$$

$$\frac{1}{2} y_2^2 \cos(\theta)^2 + \frac{1}{2} x_1^2 \sin(\theta)^2 - x_1 x_2 \sin(\theta)^2 + \frac{1}{2} x_2^2 \sin(\theta)^2$$

$$+ \frac{1}{2} y_1^2 \sin(\theta)^2 + \frac{1}{2} y_2^2 \sin(\theta)^2 - 2 x_1 \cos(\theta) \sin(\theta) +$$

$$2 x_2 \cos(\theta) \sin(\theta) + y_1 y_2 + \cos(\theta)^2 - \sin(\theta)^2$$

If $\mathbf{S}_1 = \mathbf{a}$ and $\mathbf{S}_2 = \mathbf{c}$, the dot product becomes:

$$\mathbf{S}_1 \cdot \mathbf{S}_2 = -x_1 x_2 \cos(\phi) \cos(\theta)^2 - \frac{1}{2} x_1^2 \cos(\phi) \sin(\theta)^2 - \frac{1}{2} x_2^2 \cos(\phi) \sin(\theta)^2 -$$

$$\frac{1}{2} y_1^2 \cos(\phi) \sin(\theta)^2 - \frac{1}{2} y_2^2 \cos(\phi) \sin(\theta)^2 + \frac{1}{2} x_1^2 \cos(\theta)^2 + \frac{1}{2} x_2^2 \cos(\theta)^2 +$$

$$\frac{1}{2}\, y_1^2 \cos\left(\theta\right)^2 + \frac{1}{2}\, y_2^2 \cos\left(\theta\right)^2 - x_2 y_1 \cos\left(\theta\right)\sin\left(\phi\right) - x_1 y_2 \cos\left(\theta\right)\sin\left(\phi\right) +$$

$$x_1 \cos\left(\phi\right)\cos\left(\theta\right)\sin\left(\theta\right) - x_2 \cos\left(\phi\right)\cos\left(\theta\right)\sin\left(\theta\right) +$$

$$x_1 x_2 \sin\left(\theta\right)^2 + y_1 y_2 \cos\left(\phi\right) + x_1 \cos\left(\theta\right)\sin\left(\theta\right) - x_2 \cos\left(\theta\right)\sin\left(\theta\right) +$$

$$y_1 \sin\left(\phi\right)\sin\left(\theta\right) - y_2 \sin\left(\phi\right)\sin\left(\theta\right) + \cos\left(\phi\right)\sin\left(\theta\right)^2 - \cos\left(\theta\right)^2$$

If $\mathbf{S}_1 = \mathbf{a}$ and $\mathbf{S}_2 = \mathbf{d}$, the dot product becomes:

$$\mathbf{S}_1 \cdot \mathbf{S}_2 = -x_1 x_2 \cos\left(\phi\right)\cos\left(\theta\right)^2 + \frac{1}{2}\, x_1^2 \cos\left(\phi\right)\sin\left(\theta\right)^2 + \frac{1}{2}\, x_2^2 \cos\left(\phi\right)\sin\left(\theta\right)^2 + \frac{1}{2}\, y_1^2 \cos\left(\phi\right)\sin\left(\theta\right)^2 +$$

$$\frac{1}{2}\, y_2^2 \cos\left(\phi\right)\sin\left(\theta\right)^2 + \frac{1}{2}\, x_1^2 \cos\left(\theta\right)^2 + \frac{1}{2}\, x_2^2 \cos\left(\theta\right)^2 + \frac{1}{2}\, y_1^2 \cos\left(\theta\right)^2 + \frac{1}{2}\, y_2^2 \cos\left(\theta\right)^2$$

$$- x_2 y_1 \cos\left(\theta\right)\sin\left(\phi\right) - x_1 y_2 \cos\left(\theta\right)\sin\left(\phi\right) - x_1 \cos\left(\phi\right)\cos\left(\theta\right)\sin\left(\theta\right)$$

$$- x_2 \cos\left(\phi\right)\cos\left(\theta\right)\sin\left(\theta\right) - x_1 x_2 \sin\left(\theta\right)^2 + y_1 y_2 \cos\left(\phi\right) + x_1 \cos\left(\theta\right)\sin\left(\theta\right)$$

$$+ x_2 \cos\left(\theta\right)\sin\left(\theta\right) - y_1 \sin\left(\phi\right)\sin\left(\theta\right) - y_2 \sin\left(\phi\right)\sin\left(\theta\right) - \cos\left(\phi\right)\sin\left(\theta\right)^2 - \cos\left(\theta\right)^2$$

If $\mathbf{S}_1 = \mathbf{b}$ and $\mathbf{S}_2 = \mathbf{c}$, the dot product becomes:

$$\mathbf{S}_1 \cdot \mathbf{S}_2 = -x_1 x_2 \cos\left(\phi\right)\cos\left(\theta\right)^2 + \frac{1}{2}\, x_1^2 \cos\left(\phi\right)\sin\left(\theta\right)^2 +$$

$$\frac{1}{2}\, x_2^2 \cos\left(\phi\right)\sin\left(\theta\right)^2 + \frac{1}{2}\, y_1^2 \cos\left(\phi\right)\sin\left(\theta\right)^2 + \frac{1}{2}\, y_2^2 \cos\left(\phi\right)\sin\left(\theta\right)^2 +$$

$$\frac{1}{2}\, x_1^2 \cos\left(\theta\right)^2 + \frac{1}{2}\, x_2^2 \cos\left(\theta\right)^2 +$$

$$\frac{1}{2}\, y_1^2 \cos\left(\theta\right)^2 + \frac{1}{2}\, y_2^2 \cos\left(\theta\right)^2 - x_2 y_1 \cos\left(\theta\right)\sin\left(\phi\right) -$$

$$x_1 y_2 \cos\left(\theta\right)\sin\left(\phi\right) + x_1 \cos\left(\phi\right)\cos\left(\theta\right)\sin\left(\theta\right) + x_2 \cos\left(\phi\right)\cos\left(\theta\right)\sin\left(\theta\right)$$

$$- x_1 x_2 \sin\left(\theta\right)^2 + y_1 y_2 \cos\left(\phi\right) - x_1 \cos\left(\theta\right)\sin\left(\theta\right) - x_2 \cos\left(\theta\right)\sin\left(\theta\right) +$$

$$y_1 \sin\left(\phi\right)\sin\left(\theta\right) + y_2 \sin\left(\phi\right)\sin\left(\theta\right) - \cos\left(\phi\right)\sin\left(\theta\right)^2 - \cos\left(\theta\right)^2$$

If $\mathbf{S}_1 = \mathbf{b}$ and $\mathbf{S}_2 = \mathbf{d}$, the dot product becomes:

$$\mathbf{S}_1 \cdot \mathbf{S}_2 = -x_1 x_2 \cos\left(\phi\right)\cos\left(\theta\right)^2 - \frac{1}{2}\, x_1^2 \cos\left(\phi\right)\sin\left(\theta\right)^2 - \frac{1}{2}\, x_2^2 \cos\left(\phi\right)\sin\left(\theta\right)^2 -$$

$$\frac{1}{2}\, y_1^2 \cos\left(\phi\right)\sin\left(\theta\right)^2 - \frac{1}{2}\, y_2^2 \cos\left(\phi\right)\sin\left(\theta\right)^2 +$$

$$\frac{1}{2}\, x_1^2 \cos\left(\theta\right)^2 + \frac{1}{2}\, x_2^2 \cos\left(\theta\right)^2 +$$

$$\frac{1}{2}\, y_1^2 \cos\left(\theta\right)^2 + \frac{1}{2}\, y_2^2 \cos\left(\theta\right)^2 -$$

$$x_2 y_1 \cos\left(\theta\right)\sin\left(\phi\right) - x_1 y_2 \cos\left(\theta\right)\sin\left(\phi\right) - x_1 \cos\left(\phi\right)\cos\left(\theta\right)\sin\left(\theta\right)$$

$$+ x_2 \cos{(\phi)} \cos{(\theta)} \sin{(\theta)} + x_1 x_2 \sin{(\theta)}^2 + y_1 y_2 \cos{(\phi)} -$$
$$x_1 \cos{(\theta)} \sin{(\theta)} + x_2 \cos{(\theta)} \sin{(\theta)}$$
$$- y_1 \sin{(\phi)} \sin{(\theta)} + y_2 \sin{(\phi)} \sin{(\theta)} + \cos{(\phi)} \sin{(\theta)}^2 - \cos{(\theta)}^2$$

If $\mathbf{S}_1 = \mathbf{c}$ and $\mathbf{S}_2 = \mathbf{d}$, the dot product becomes:

$$\mathbf{S}_1 \cdot \mathbf{S}_2 = x_1 x_2 \cos{(\phi)}^2 \cos{(\theta)}^2 + x_1 x_2 \cos{(\theta)}^2 \sin{(\phi)}^2 + \frac{1}{2} x_1^2 \cos{(\phi)}^2 \sin{(\theta)}^2 +$$

$$\frac{1}{2} x_2^2 \cos{(\phi)}^2 \sin{(\theta)}^2 + \frac{1}{2} y_1^2 \cos{(\phi)}^2 \sin{(\theta)}^2 + \frac{1}{2} y_2^2 \cos{(\phi)}^2 \sin{(\theta)}^2 +$$

$$\frac{1}{2} x_1^2 \sin{(\phi)}^2 \sin{(\theta)}^2 + \frac{1}{2} x_2^2 \sin{(\phi)}^2 \sin{(\theta)}^2 + \frac{1}{2} y_1^2 \sin{(\phi)}^2 \sin{(\theta)}^2 +$$

$$\frac{1}{2} y_2^2 \sin{(\phi)}^2 \sin{(\theta)}^2 + x_1 \cos{(\phi)}^2 \cos{(\theta)} \sin{(\theta)} - x_2 \cos{(\phi)}^2 \cos{(\theta)} \sin{(\theta)} +$$

$$x_1 \cos{(\theta)} \sin{(\phi)}^2 \sin{(\theta)} - x_2 \cos{(\theta)} \sin{(\phi)}^2 \sin{(\theta)} + y_1 y_2 \cos{(\phi)}^2 - \frac{1}{2} x_1^2 \cos{(\theta)}^2$$

$$- \frac{1}{2} x_2^2 \cos{(\theta)}^2 - \frac{1}{2} y_1^2 \cos{(\theta)}^2 - \frac{1}{2} y_2^2 \cos{(\theta)}^2 + y_1 y_2 \sin{(\phi)}^2$$
$$- x_1 x_2 \sin{(\theta)}^2 - \cos{(\phi)}^2 \sin{(\theta)}^2 - \sin{(\phi)}^2 \sin{(\theta)}^2 +$$
$$x_1 \cos{(\theta)} \sin{(\theta)} - x_2 \cos{(\theta)} \sin{(\theta)} + \cos{(\theta)}^2$$

In order to further simplify notation, we use numbers for the first two indices as well. Here, having index the first index equal to 1 means that the first index is j. If it is 0 it is equal to $j - 1$, and 2 means it's equal to $j + 1$. The same applies to the l index. Inserting the dot products in the Hamiltonian, we get:

$$H = \sum_j -\frac{1}{4} (J_1 \cos(\phi) - J_1) x_{01111}^2 \sin(\theta)^2 + \frac{1}{4} (J_1 \cos(\phi) + J_1) x_{01121}^2 \sin(\theta)^2 -$$

$$\frac{1}{4} (J_1 \cos(\phi) - J_1) x_{01131}^2 \sin(\theta)^2 - \frac{1}{4} (J_1 \cos(\phi) - 3 J_1) x_{11130}^2 \sin(\theta)^2 -$$

$$\frac{1}{4} (J_1 \cos(\phi) - J_1) y_{01111}^2 \sin(\theta)^2 + \frac{1}{4} (J_1 \cos(\phi) + J_1) y_{01121}^2 \sin(\theta)^2 -$$

$$\frac{1}{4} (J_1 \cos(\phi) - J_1) y_{01131}^2 \sin(\theta)^2 - \frac{1}{4} (J_1 \cos(\phi) - 3 J_1) y_{11130}^2 \sin(\theta)^2 -$$

$$J_1 x_{01100} \cos(\theta) \sin(\theta) + J_1 x_{01101} \cos(\theta) \sin(\theta) -$$

$$\frac{1}{2} (J_1 \cos(\phi) - J_1) x_{01110} \cos(\theta) \sin(\theta) - \frac{1}{2} (J_1 \cos(\phi) - J_1) x_{01111} \cos(\theta) \sin(\theta) -$$

$$\frac{1}{2} (J_1 \cos(\phi) + J_1) x_{01120} \cos(\theta) \sin(\theta) - \frac{1}{2} (J_1 \cos(\phi) + J_1) x_{01121} \cos(\theta) \sin(\theta) +$$

$$\frac{1}{2}\left(J_1\cos(\phi)-J_1\right)x_{01130}\cos(\theta)\sin(\theta)+\frac{1}{2}\left(J_1\cos(\phi)-J_1\right)x_{01131}\cos(\theta)\sin(\theta)+$$

$$\frac{1}{2}\left(J_1\cos(\phi)+3\,J_1\right)x_{02100}\cos(\theta)\sin(\theta)+\frac{1}{2}\left(J_1\cos(\phi)-J_1\right)x_{02101}\cos(\theta)\sin(\theta)+$$

$$\frac{1}{2}\left(J_1\cos(\phi)+J_1\right)x_{10030}\cos(\theta)\sin(\theta)+\frac{1}{2}\left(J_1\cos(\phi)-3\,J_1\right)x_{10031}\cos(\theta)\sin(\theta)-$$

$$J_1x_{10130}\cos(\theta)\sin(\theta)+3\,J_1x_{10131}\cos(\theta)\sin(\theta)+\frac{1}{4}\left(2\,J_1\sin(\theta)^2-J_1\right)x_{01100}^2+$$

$$\frac{1}{4}\left(2\,J_1\sin(\theta)^2-J_1\right)x_{01101}^2+\frac{1}{4}\left((J_1\cos(\phi)-J_1)\sin(\theta)^2+2\,J_1\right)x_{01110}^2-$$

$$\frac{1}{4}\left((J_1\cos(\phi)+J_1)\sin(\theta)^2-2\,J_1\right)x_{01120}^2+\frac{1}{4}\left((J_1\cos(\phi)-J_1)\sin(\theta)^2+2\,J_1\right)x_{01130}^2-$$

$$\frac{1}{4}\left((J_1\cos(\phi)+3\,J_1)\sin(\theta)^2-3\,J_1\right)x_{02100}^2+\frac{1}{4}\left((J_1\cos(\phi)-J_1)\sin(\theta)^2+J_1\right)x_{02101}^2-$$

$$\frac{1}{4}\left((J_1\cos(\phi)+J_1)\sin(\theta)^2-J_1\right)x_{10030}^2+\frac{1}{4}\left((J_1\cos(\phi)-3\,J_1)\sin(\theta)^2+3\,J_1\right)x_{10031}^2-$$

$$\frac{1}{2}\left(J_1\sin(\theta)^2-J_1\right)x_{10130}^2-\frac{3}{2}\left(J_1\sin(\theta)^2-J_1\right)x_{10131}^2+$$

$$J_1x_{11000}^2+J_1x_{11001}^2+J_1x_{11010}^2+J_1x_{11011}^2+J_1x_{11020}^2+J_1x_{11021}^2+$$

$$\frac{1}{4}\left((J_1\cos(\phi)+J_1)\sin(\theta)^2+3\,J_1\right)x_{11030}^2-\frac{1}{4}\left((J_1\cos(\phi)-3\,J_1)\sin(\theta)^2-J_1\right)x_{11031}^2+$$

$$\frac{1}{4}\left((J_1\cos(\phi)+J_1)\sin(\theta)^2+2\,J_1\right)x_{11100}^2-\frac{1}{4}\left((J_1\cos(\phi)+J_1)\sin(\theta)^2-4\,J_1\right)x_{11101}^2-$$

$$\frac{1}{4}\left((J_1\cos(\phi)-J_1)\sin(\theta)^2-2\,J_1\right)x_{11110}^2+\frac{1}{4}\left((J_1\cos(\phi)-J_1)\sin(\theta)^2+4\,J_1\right)x_{11111}^2+$$

$$\frac{1}{4}\left((J_1\cos(\phi)+J_1)\sin(\theta)^2+2\,J_1\right)x_{11120}^2-\frac{1}{4}\left((J_1\cos(\phi)+J_1)\sin(\theta)^2-4\,J_1\right)x_{11121}^2+$$

$$\frac{1}{4}\left((J_1\cos(\phi)+5\,J_1)\sin(\theta)^2-2\,J_1\right)x_{11131}^2+\frac{1}{4}\left(2\,J_1\sin(\theta)^2-J_1\right)y_{01100}^2+$$

$$\frac{1}{4}\left(2\,J_1\sin(\theta)^2-J_1\right)y_{01101}^2+\frac{1}{4}\left((J_1\cos(\phi)-J_1)\sin(\theta)^2+2\,J_1\right)y_{01110}^2-$$

$$\frac{1}{4}\left((J_1\cos(\phi)+J_1)\sin(\theta)^2-2\,J_1\right)y_{01120}^2+\frac{1}{4}\left((J_1\cos(\phi)-J_1)\sin(\theta)^2+2\,J_1\right)y_{01130}^2-$$

$$\frac{1}{4}\left((J_1\cos(\phi)+3\,J_1)\sin(\theta)^2-3\,J_1\right)y_{02100}^2+\frac{1}{4}\left((J_1\cos(\phi)-J_1)\sin(\theta)^2+J_1\right)y_{02101}^2-$$

$$\frac{1}{4}\left((J_1\cos(\phi)+J_1)\sin(\theta)^2-J_1\right)y_{10030}^2+\frac{1}{4}\left((J_1\cos(\phi)-3\,J_1)\sin(\theta)^2+3\,J_1\right)y_{10031}^2-$$

$$\frac{1}{2}\left(J_1\sin(\theta)^2-J_1\right)y_{10130}^2-\frac{3}{2}\left(J_1\sin(\theta)^2-J_1\right)y_{10131}^2+$$

$$J_1y_{11000}^2+J_1y_{11001}^2+J_1y_{11010}^2+J_1y_{11011}^2+J_1y_{11020}^2+J_1y_{11021}^2+$$

$$\frac{1}{4}\left((J_1\cos(\phi)+J_1)\sin(\theta)^2+3\,J_1\right)y_{11030}^2-\frac{1}{4}\left((J_1\cos(\phi)-3\,J_1)\sin(\theta)^2-J_1\right)y_{11031}^2+$$

$$\frac{1}{4}\left((J_1\cos(\phi)+J_1)\sin(\theta)^2+2\,J_1\right)y_{11100}^2-\frac{1}{4}\left((J_1\cos(\phi)+J_1)\sin(\theta)^2-4\,J_1\right)y_{11101}^2-$$

$$\frac{1}{4}\left((J_1\cos(\phi)-J_1)\sin(\theta)^2-2\,J_1\right)y_{11110}^2+\frac{1}{4}\left((J_1\cos(\phi)-J_1)\sin(\theta)^2+4\,J_1\right)y_{11111}^2+$$

$$\frac{1}{4}\left((J_1\cos(\phi)+J_1)\sin(\theta)^2+2\,J_1\right)y_{11120}^2-\frac{1}{4}\left((J_1\cos(\phi)+J_1)\sin(\theta)^2-4\,J_1\right)y_{11121}^2+$$

$$\frac{1}{4}\left((J_1\cos(\phi)+5\,J_1)\sin(\theta)^2-2\,J_1\right)y_{11131}^2-\frac{1}{2}\left((2\,J_1\sin(\theta)^2-J_1)x_{01100}\right.$$

$$-\,((J_1\cos(\phi)+J_1)\sin(\theta)^2-J_1\cos(\phi))x_{01110}-((J_1\cos(\phi)+J_1)\sin(\theta)^2-J_1\cos(\phi))x_{10030}-$$

$$2\,((J_1\cos(\phi)-J_1)\sin(\theta)^2-J_1\cos(\phi))x_{10031}-((J_1\cos(\phi)-J_1)\sin(\theta)^2-J_1\cos(\phi))x_{10130}-$$

$$2\,((J_1\cos(\phi)+J_1)\sin(\theta)^2-J_1\cos(\phi))x_{10131})x_{11000}-\frac{1}{2}\left((2\,J_1\sin(\theta)^2-J_1)x_{01101}-\right.$$

$$2\,((J_1\cos(\phi)-J_1)\sin(\theta)^2-J_1\cos(\phi))x_{01110}-((J_1\cos(\phi)+J_1)\sin(\theta)^2-J_1\cos(\phi))x_{01111}-$$

$$((J_1\cos(\phi)+J_1)\sin(\theta)^2-J_1\cos(\phi))x_{10031}-((J_1\cos(\phi)-J_1)\sin(\theta)^2-J_1\cos(\phi))x_{10131}$$

$$+\,2\,(2\,J_1\sin(\theta)^2-J_1)x_{11000})x_{11001}-\frac{1}{2}\left((2\,J_1\sin(\theta)^2-J_1)x_{01110}-\right.$$

$$((J_1\cos(\phi)-J_1)\sin(\theta)^2-J_1\cos(\phi))x_{01120}-((J_1\cos(\phi)-J_1)\sin(\theta)^2-J_1\cos(\phi))x_{11000}-$$

$$2\,((J_1\cos(\phi)+J_1)\sin(\theta)^2-J_1\cos(\phi))x_{11001})x_{11010}-\frac{1}{2}\left((2\,J_1\sin(\theta)^2-J_1)x_{01111}\right.$$

$$-\,2\,((J_1\cos(\phi)+J_1)\sin(\theta)^2-J_1\cos(\phi))x_{01120}-((J_1\cos(\phi)-J_1)\sin(\theta)^2-J_1\cos(\phi))x_{01121}-$$

$$((J_1\cos(\phi)-J_1)\sin(\theta)^2-J_1\cos(\phi))x_{11001}+2\,(2\,J_1\sin(\theta)^2-J_1)x_{11010})x_{11011}$$

$$-\,\frac{1}{2}\left((2\,J_1\sin(\theta)^2-J_1)x_{01120}-((J_1\cos(\phi)+J_1)\sin(\theta)^2-J_1\cos(\phi))x_{01130}\right.$$

$$-\,((J_1\cos(\phi)+J_1)\sin(\theta)^2-J_1\cos(\phi))x_{11010}-2\,((J_1\cos(\phi)-J_1)\sin(\theta)^2-J_1\cos(\phi))x_{11011})x_{11020}$$

$$-\,\frac{1}{2}\left((2\,J_1\sin(\theta)^2-J_1)x_{01121}-2\,((J_1\cos(\phi)-J_1)\sin(\theta)^2-J_1\cos(\phi))x_{01130}-\right.$$

$$((J_1\cos(\phi)+J_1)\sin(\theta)^2-J_1\cos(\phi))x_{01131}-((J_1\cos(\phi)+J_1)\sin(\theta)^2-J_1\cos(\phi))x_{11011}+$$

$$2\,(2\,J_1\sin(\theta)^2-J_1)x_{11020})x_{11021}-\frac{1}{2}\left(((J_1\cos(\phi)+J_1)\cos(\theta)\sin(\theta)+(2\,J_1\sin(\theta)^2-J_1)x_{01130}-\right.$$

$$((J_1\cos(\phi)-J_1)\sin(\theta)^2-J_1\cos(\phi))x_{02100}-((J_1\cos(\phi)-J_1)\sin(\theta)^2-J_1\cos(\phi))x_{11020}-$$

$$2\,((J_1\cos(\phi)+J_1)\sin(\theta)^2-J_1\cos(\phi))x_{11021})x_{11030}-$$

$$\frac{1}{2}\left(((J_1\cos(\phi)-3\,J_1)\cos(\theta)\sin(\theta)+(2\,J_1\sin(\theta)^2-J_1)x_{01131}\right.$$

$$-\,2\,((J_1\cos(\phi)+J_1)\sin(\theta)^2-J_1\cos(\phi))x_{02100}-((J_1\cos(\phi)-J_1)\sin(\theta)^2-J_1\cos(\phi))x_{02101}-$$

$$((J_1\cos(\phi)-J_1)\sin(\theta)^2-J_1\cos(\phi))x_{11021}+2\,(2\,J_1\sin(\theta)^2-J_1)x_{11030})x_{11031}$$

32

$$-\frac{1}{2}\left((J_1\cos(\phi)+J_1)\cos(\theta)\sin(\theta)-((J_1\cos(\phi)+J_1)\sin(\theta)^2-J_1\cos(\phi))x_{10130}-\right.$$
$$2\left((J_1\cos(\phi)-J_1)\sin(\theta)^2-J_1\cos(\phi)\right)x_{10131}+(2J_1\sin(\theta)^2-J_1)x_{11000}-$$
$$((J_1\cos(\phi)+J_1)\sin(\theta)^2-J_1\cos(\phi))x_{11010})x_{11100}-$$
$$\frac{1}{2}\left((J_1\cos(\phi)+J_1)\cos(\theta)\sin(\theta)-((J_1\cos(\phi)+J_1)\sin(\theta)^2-J_1\cos(\phi))x_{10131}\right.$$
$$+\left(2J_1\sin(\theta)^2-J_1\right)x_{11001}-2\left((J_1\cos(\phi)-J_1)\sin(\theta)^2-J_1\cos(\phi)\right)x_{11010}$$
$$-((J_1\cos(\phi)+J_1)\sin(\theta)^2-J_1\cos(\phi))x_{11011}+$$
$$2\left(2J_1\sin(\theta)^2-J_1\right)x_{11100})x_{11101}$$
$$+\frac{1}{2}\left((J_1\cos(\phi)-J_1)\cos(\theta)\sin(\theta)-(2J_1\sin(\theta)^2-J_1)x_{11010}+\right.$$
$$((J_1\cos(\phi)-J_1)\sin(\theta)^2-J_1\cos(\phi))x_{11020}$$
$$+\left((J_1\cos(\phi)-J_1)\sin(\theta)^2-J_1\cos(\phi)\right)x_{11100}+2\left((J_1\cos(\phi)+J_1)\sin(\theta)^2-J_1\cos(\phi)\right)x_{11101})x_{11110}$$
$$+\frac{1}{2}\left((J_1\cos(\phi)-J_1)\cos(\theta)\sin(\theta)-(2J_1\sin(\theta)^2-J_1)x_{11011}+\right.$$
$$2\left((J_1\cos(\phi)+J_1)\sin(\theta)^2-J_1\cos(\phi)\right)x_{11020}+$$
$$((J_1\cos(\phi)-J_1)\sin(\theta)^2-J_1\cos(\phi))x_{11021}+((J_1\cos(\phi)-J_1)\sin(\theta)^2-J_1\cos(\phi))x_{11101}-$$
$$2\left(2J_1\sin(\theta)^2-J_1\right)x_{11110})x_{11111}+\frac{1}{2}\left((J_1\cos(\phi)+J_1)\cos(\theta)\sin(\theta)-(2J_1\sin(\theta)^2-J_1)x_{11020}+\right.$$
$$((J_1\cos(\phi)+J_1)\sin(\theta)^2-J_1\cos(\phi))x_{11030}+((J_1\cos(\phi)+J_1)\sin(\theta)^2-J_1\cos(\phi))x_{11110}+$$
$$2\left((J_1\cos(\phi)-J_1)\sin(\theta)^2-J_1\cos(\phi)\right)x_{11111})x_{11120}+$$
$$\frac{1}{2}\left((J_1\cos(\phi)+J_1)\cos(\theta)\sin(\theta)-(2J_1\sin(\theta)^2-J_1)x_{11021}\right.$$
$$+2\left((J_1\cos(\phi)-J_1)\sin(\theta)^2-J_1\cos(\phi)\right)x_{11030}+$$
$$((J_1\cos(\phi)+J_1)\sin(\theta)^2-J_1\cos(\phi))x_{11031}+((J_1\cos(\phi)+J_1)\sin(\theta)^2-J_1\cos(\phi))x_{11111}-$$
$$2\left(2J_1\sin(\theta)^2-J_1\right)x_{11120})x_{11121}-$$
$$\frac{1}{2}\left((J_1\cos(\phi)-3J_1)\cos(\theta)\sin(\theta)+(2J_1\sin(\theta)^2-J_1)x_{11030}-\right.$$
$$((J_1\cos(\phi)-J_1)\sin(\theta)^2-J_1\cos(\phi))x_{11120}$$
$$-2\left((J_1\cos(\phi)+J_1)\sin(\theta)^2-J_1\cos(\phi)\right)x_{11121})x_{11130}-$$
$$\frac{1}{2}\left((J_1\cos(\phi)+5J_1)\cos(\theta)\sin(\theta)+(2J_1\sin(\theta)^2-J_1)x_{11031}\right.$$
$$-((J_1\cos(\phi)-J_1)\sin(\theta)^2-J_1\cos(\phi))x_{11121}+2\left(2J_1\sin(\theta)^2-J_1\right)x_{11130})x_{11131}$$

$$-\frac{1}{2}\left(J_1x_{11000}\cos(\theta)\sin(\phi)+2J_1x_{11001}\cos(\theta)\sin(\phi)+\right.$$

$$J_1 \sin(\phi)\sin(\theta))y_{01110} - \frac{1}{2}\left(J_1 x_{11001}\cos(\theta)\sin(\phi) + J_1\sin(\phi)\sin(\theta)\right)y_{01111}$$

$$-\frac{1}{2}\left(J_1 x_{11010}\cos(\theta)\sin(\phi) + 2\,J_1 x_{11011}\cos(\theta)\sin(\phi) + J_1\sin(\phi)\sin(\theta)\right)y_{01120} -$$

$$\frac{1}{2}\left(J_1 x_{11011}\cos(\theta)\sin(\phi) + J_1\sin(\phi)\sin(\theta)\right)y_{01121} - \frac{1}{2}\left(J_1 x_{11020}\cos(\theta)\sin(\phi) + \right.$$

$$2\,J_1 x_{11021}\cos(\theta)\sin(\phi) - J_1\sin(\phi)\sin(\theta))y_{01130} - \frac{1}{2}\left(J_1 x_{11021}\cos(\theta)\sin(\phi) - \right.$$

$$J_1\sin(\phi)\sin(\theta))y_{01131} - \frac{1}{2}\left(J_1 x_{11030}\cos(\theta)\sin(\phi) + 2\,J_1 x_{11031}\cos(\theta)\sin(\phi) - \right.$$

$$J_1\sin(\phi)\sin(\theta))y_{02100} - \frac{1}{2}\left(J_1 x_{11031}\cos(\theta)\sin(\phi) - J_1\sin(\phi)\sin(\theta)\right)y_{02101} -$$

$$\frac{1}{2}\left(J_1 x_{11000}\cos(\theta)\sin(\phi) - J_1\sin(\phi)\sin(\theta)\right)y_{10030} -$$

$$\frac{1}{2}\left(2\,J_1 x_{11000}\cos(\theta)\sin(\phi) + J_1 x_{11001}\cos(\theta)\sin(\phi) - J_1\sin(\phi)\sin(\theta)\right)y_{10031}$$

$$-\frac{1}{2}\left(J_1 x_{11000}\cos(\theta)\sin(\phi) + J_1 x_{11100}\cos(\theta)\sin(\phi)\right)y_{10130} -$$

$$\frac{1}{2}\left(2\,J_1 x_{11000}\cos(\theta)\sin(\phi) + J_1 x_{11001}\cos(\theta)\sin(\phi) + \right.$$

$$2\,J_1 x_{11100}\cos(\theta)\sin(\phi) + J_1 x_{11101}\cos(\theta)\sin(\phi))y_{10131} -$$

$$\frac{1}{2}\left(J_1 x_{01110}\cos(\theta)\sin(\phi) + J_1 x_{10030}\cos(\theta)\sin(\phi) + 2\,J_1 x_{10031}\cos(\theta)\sin(\phi)\right.$$

$$+ J_1 x_{10130}\cos(\theta)\sin(\phi) + 2\,J_1 x_{10131}\cos(\theta)\sin(\phi) + J_1 x_{11010}\cos(\theta)\sin(\phi)$$

$$- J_1 y_{01110}\cos(\phi) - J_1 y_{10030}\cos(\phi) - 2\,J_1 y_{10031}\cos(\phi)$$

$$- J_1 y_{10130}\cos(\phi) - 2\,J_1 y_{10131}\cos(\phi) - J_1 y_{01100})y_{11000}$$

$$-\frac{1}{2}\left(2\,J_1 x_{01110}\cos(\theta)\sin(\phi) + J_1 x_{01111}\cos(\theta)\sin(\phi) + J_1 x_{10031}\cos(\theta)\sin(\phi)\right.$$

$$+ J_1 x_{10131}\cos(\theta)\sin(\phi) + 2\,J_1 x_{11010}\cos(\theta)\sin(\phi) + J_1 x_{11011}\cos(\theta)\sin(\phi)$$

$$- 2\,J_1 y_{01110}\cos(\phi) - J_1 y_{01111}\cos(\phi) - J_1 y_{10031}\cos(\phi)$$

$$- J_1 y_{10131}\cos(\phi) - J_1 y_{01101} - 2\,J_1 y_{11000})y_{11001}$$

$$-\frac{1}{2}\left(J_1 x_{01120}\cos(\theta)\sin(\phi) + J_1 x_{11000}\cos(\theta)\sin(\phi) + 2\,J_1 x_{11001}\cos(\theta)\sin(\phi)\right.$$

$$+ J_1 x_{11020}\cos(\theta)\sin(\phi) + J_1 x_{11100}\cos(\theta)\sin(\phi) +$$

$$2\,J_1 x_{11101}\cos(\theta)\sin(\phi) - J_1 y_{01120}\cos(\phi) - J_1 y_{11000}\cos(\phi) -$$

$$2\,J_1 y_{11001}\cos(\phi) - J_1 y_{01110})y_{11010} - \frac{1}{2}\left(2\,J_1 x_{01120}\cos(\theta)\sin(\phi) + \right.$$

$$J_1 x_{01121}\cos(\theta)\sin(\phi) + J_1 x_{11001}\cos(\theta)\sin(\phi) + 2\,J_1 x_{11020}\cos(\theta)\sin(\phi) +$$

$$J_1 x_{11021} \cos(\theta)\sin(\phi) + J_1 x_{11101}\cos(\theta)\sin(\phi) - 2\,J_1 y_{01120}\cos(\phi)-$$

$$J_1 y_{01121}\cos(\phi) - J_1 y_{11001}\cos(\phi) - J_1 y_{01111} - 2\,J_1 y_{11010})y_{11011}$$

$$-\frac{1}{2}\left(J_1 x_{01130}\cos(\theta)\sin(\phi) + J_1 x_{11010}\cos(\theta)\sin(\phi) + 2\,J_1 x_{11011}\cos(\theta)\sin(\phi)+\right.$$

$$J_1 x_{11030}\cos(\theta)\sin(\phi) + J_1 x_{11110}\cos(\theta)\sin(\phi) + 2\,J_1 x_{11111}\cos(\theta)\sin(\phi)-$$

$$\left. J_1 y_{01130}\cos(\phi) - J_1 y_{11010}\cos(\phi) - 2\,J_1 y_{11011}\cos(\phi) - J_1 y_{01120}\right)y_{11020}$$

$$-\frac{1}{2}\left(2\,J_1 x_{01130}\cos(\theta)\sin(\phi) + J_1 x_{01131}\cos(\theta)\sin(\phi) + J_1 x_{11011}\cos(\theta)\sin(\phi)+\right.$$

$$2\,J_1 x_{11030}\cos(\theta)\sin(\phi) + J_1 x_{11031}\cos(\theta)\sin(\phi) + J_1 x_{11111}\cos(\theta)\sin(\phi)-$$

$$\left. 2\,J_1 y_{01130}\cos(\phi) - J_1 y_{01131}\cos(\phi) - J_1 y_{11011}\cos(\phi) - J_1 y_{01121} - 2\,J_1 y_{11020}\right)y_{11021}$$

$$-\frac{1}{2}\left(J_1 x_{02100}\cos(\theta)\sin(\phi) + J_1 x_{11020}\cos(\theta)\sin(\phi) + 2\,J_1 x_{11021}\cos(\theta)\sin(\phi) + J_1 x_{11120}\cos(\theta)\sin(\phi)\right.$$

$$+ 2\,J_1 x_{11121}\cos(\theta)\sin(\phi) - J_1 y_{02100}\cos(\phi) - J_1 y_{11020}\cos(\phi)-$$

$$\left. 2\,J_1 y_{11021}\cos(\phi) + J_1 \sin(\phi)\sin(\theta) - J_1 y_{01130}\right)y_{11030}$$

$$-\frac{1}{2}\left(2\,J_1 x_{02100}\cos(\theta)\sin(\phi) + J_1 x_{02101}\cos(\theta)\sin(\phi) + J_1 x_{11021}\cos(\theta)\sin(\phi)+\right.$$

$$J_1 x_{11121}\cos(\theta)\sin(\phi) - 2\,J_1 y_{02100}\cos(\phi) - J_1 y_{02101}\cos(\phi)-$$

$$\left. J_1 y_{11021}\cos(\phi) + J_1 \sin(\phi)\sin(\theta) - J_1 y_{01131} - 2\,J_1 y_{11030}\right)y_{11031}-$$

$$\frac{1}{2}\left(J_1 x_{10130}\cos(\theta)\sin(\phi) + 2\,J_1 x_{10131}\cos(\theta)\sin(\phi) + J_1 x_{11010}\cos(\theta)\sin(\phi)+\right.$$

$$J_1 x_{11110}\cos(\theta)\sin(\phi) - J_1 y_{10130}\cos(\phi) - 2\,J_1 y_{10131}\cos(\phi)-$$

$$\left. J_1 y_{11010}\cos(\phi) + J_1 \sin(\phi)\sin(\theta) - J_1 y_{11000}\right)y_{11100}-$$

$$\frac{1}{2}\left(J_1 x_{10131}\cos(\theta)\sin(\phi) + 2\,J_1 x_{11010}\cos(\theta)\sin(\phi) + J_1 x_{11011}\cos(\theta)\sin(\phi)+\right.$$

$$2\,J_1 x_{11110}\cos(\theta)\sin(\phi) + J_1 x_{11111}\cos(\theta)\sin(\phi) - J_1 y_{10131}\cos(\phi)-$$

$$\left. 2\,J_1 y_{11010}\cos(\phi) - J_1 y_{11011}\cos(\phi) + J_1 \sin(\phi)\sin(\theta) - J_1 y_{11001} - 2\,J_1 y_{11100}\right)y_{11101}-$$

$$\frac{1}{2}\left(J_1 x_{11020}\cos(\theta)\sin(\phi) + J_1 x_{11100}\cos(\theta)\sin(\phi) + 2\,J_1 x_{11101}\cos(\theta)\sin(\phi)+\right.$$

$$J_1 x_{11120}\cos(\theta)\sin(\phi) - J_1 y_{11020}\cos(\phi) - J_1 y_{11100}\cos(\phi)-$$

$$\left. 2\,J_1 y_{11101}\cos(\phi) - J_1 \sin(\phi)\sin(\theta) - J_1 y_{11010}\right)y_{11110}-$$

$$\frac{1}{2}\left(2\,J_1 x_{11020}\cos(\theta)\sin(\phi) + J_1 x_{11021}\cos(\theta)\sin(\phi) + J_1 x_{11101}\cos(\theta)\sin(\phi)+\right.$$

$$2\,J_1 x_{11120}\cos(\theta)\sin(\phi) + J_1 x_{11121}\cos(\theta)\sin(\phi) - 2\,J_1 y_{11020}\cos(\phi)-$$

$$J_1 y_{11021}\cos(\phi) - J_1 y_{11101}\cos(\phi) - J_1 \sin(\phi)\sin(\theta) - J_1 y_{11011}$$

$$\left. - 2\,J_1 y_{11110}\right)y_{11111} - \frac{1}{2}\left(J_1 x_{11030}\cos(\theta)\sin(\phi) + J_1 x_{11110}\cos(\theta)\sin(\phi)+\right.$$

$2\,J_1 x_{11111}\cos(\theta)\sin(\phi) + J_1 x_{11130}\cos(\theta)\sin(\phi) - J_1 y_{11030}\cos(\phi)$

$\quad - J_1 y_{11110}\cos(\phi) - 2\,J_1 y_{11111}\cos(\phi) - J_1\sin(\phi)\sin(\theta) - J_1 y_{11020})y_{11120}-$

$\dfrac{1}{2}\,(2\,J_1 x_{11030}\cos(\theta)\sin(\phi) + J_1 x_{11031}\cos(\theta)\sin(\phi) + J_1 x_{11111}\cos(\theta)\sin(\phi)+$

$2\,J_1 x_{11130}\cos(\theta)\sin(\phi) + J_1 x_{11131}\cos(\theta)\sin(\phi) - 2\,J_1 y_{11030}\cos(\phi)-$

$J_1 y_{11031}\cos(\phi) - J_1 y_{11111}\cos(\phi) - J_1\sin(\phi)\sin(\theta) - J_1 y_{11021} - 2\,J_1 y_{11120})y_{11121}-$

$\dfrac{1}{2}\,(J_1 x_{11120}\cos(\theta)\sin(\phi) + 2\,J_1 x_{11121}\cos(\theta)\sin(\phi) - J_1 y_{11120}\cos(\phi)-$

$2\,J_1 y_{11121}\cos(\phi) + J_1\sin(\phi)\sin(\theta) - J_1 y_{11030})y_{11130}$

$\quad -\dfrac{1}{2}\,(J_1 x_{11121}\cos(\theta)\sin(\phi) - J_1 y_{11121}\cos(\phi) + J_1\sin(\phi)\sin(\theta) - J_1 y_{11031} - 2\,J_1 y_{11130})y_{11131} - 16\,J_1$

Although the Fourier transform was also done analytically, the detailed expression obtained from the Fourier transform of the Hamiltonian and the resulting 32×32 matrix is not given here, but can be obtained straightforwardly by applying the rules in eq. 29 to the given Hamiltonian, or by requesting the program used for the symbolic calculations from the author.